

Multilevel Diffusion: Infinite Dimensional Score-Based Diffusion Models for Image Generation *

Paul Hagemann [†], Sophie Mildenerger[†], Lars Ruthotto [‡], Gabriele Steidl [†], and Nicole Tianjiao Yang [‡]

Abstract. Score-based diffusion models (SBDM) have recently emerged as state-of-the-art approaches for image generation. Existing SBDMs are typically formulated in a finite-dimensional setting, where images are considered as tensors of finite size. This paper develops SBDMs in the infinite-dimensional setting, that is, we model the training data as functions supported on a rectangular domain. Besides the quest for generating images at ever higher resolution, our primary motivation is to create a well-posed infinite-dimensional learning problem so that we can discretize it consistently on multiple resolution levels. We thereby intend to obtain diffusion models that generalize across different resolution levels and improve the efficiency of the training process. We demonstrate how to overcome two shortcomings of current SBDM approaches in the infinite-dimensional setting. First, we modify the forward process to ensure that the latent distribution is well-defined in the infinite-dimensional setting using the notion of trace class operators. We derive the reverse processes for finite approximations. Second, we illustrate that approximating the score function with an operator network is beneficial for multilevel training. After deriving the convergence of the discretization and the approximation of multilevel training, we implement an infinite-dimensional SBDM approach and show the first promising results on MNIST and Fashion-MNIST, underlining our developed theory.

Key words. Generative modeling, score-based diffusion models, infinite-dimensional SDEs, neural operator

MSC codes. 60H10, 65D18

1. Introduction. Score-based diffusion models (SBDMs), first introduced in [55], have achieved impressive results in high dimensional image generation [28, 57]. The papers [30, 58] provided the underlying theoretical foundations by leveraging the probabilistic foundations of diffusion models. In [56], it was shown that for each diffusion model, there is a continuous normalizing flow that produces the same marginals, enabling exact likelihood matching.

Most, if not all, existing SBDMs for image generation interpret the training data as tensors that consist of a finite number of pixels or voxels and a few channels. This finite-dimensional viewpoint and the resulting learning schemes have recently emerged as state-of-the-art approaches for image generation and produced impressive results; see, e.g., [48, 58].

In this paper, we model the training data as functions supported on a rectangular domain and extend SBDMs to function spaces, in our case, a separable Hilbert space. There is keen interest in generating high-resolution images; hence, an ill-posed infinite-dimensional formulation could limit progress in this area. Further, similar abstractions from discrete to continuous have, for example, led to new neural network architectures motivated by ODEs

*Submitted to the editors Nov 3, 2023.

Funding: NY and LR's work was supported in part by NSF awards DMS 1751636, DMS 2038118, AFOSR grant FA9550-20-1-0372, and US DOE Office of Advanced Scientific Computing Research Field Work Proposal 20-023231. PH and GS gratefully acknowledge funding within the DFG-SPP 2298 „Theoretical Foundations of Deep Learning”.

[†]TU Berlin (E-mail: {hagemann, steidl}@math.tu-berlin.de, mildenerger@tu-berlin.de)

[‡]Department of Mathematics, Emory University, Atlanta, GA (E-mail: {lruthotto, tyang31}@emory.edu)

and PDEs [11, 21, 8, 50] and created the field of PDE-based image processing, which has generated new insights, models, and algorithms in the last decades [7]. Third, a well-posed infinite-dimensional problem and a suitable discretization can have practical advantages. For example, it allows one to approximate the solutions of the infinite-dimensional problem by using a coarse-to-fine hierarchy of resolution levels, thereby lowering computational costs.

As shown below, the extension and interpretation of SBDMs in the infinite limit is non-trivial, and we tackle several theoretical challenges.

Contributions and main results. Existing SBDMs use a standard Gaussian as a latent distribution, which is not well defined in the infinite-dimensional setting. To overcome this issue, we choose a Gaussian with a trace class covariance operator as the latent distribution and modify the forward and reverse process accordingly. We show that the finite forward stochastic differential equation possesses a well-defined limit as the solution of a Hilbert space-valued stochastic differential equation. The reverse equation is trickier to handle in the presence of the infinite-dimensional score. We circumvent this technical issue by considering the limit of the finite-dimensional discrete stochastic differential equations and the reverse SDE theory [15]. With this approach, we retain weak convergence guarantees.

We give an approximation result for replacing the reverse score with a learned neural network and show that under Lipschitz conditions, the path measures of the forward and reverse SDE are close; see [Theorem 3.6](#). To motivate multilevel training, we also prove in [Theorem 3.8](#) that training on coarse scores yields good approximations on finer levels.

We experimentally compare three trace class priors to the standard Gaussian and compare commonly used U-Nets to a neural operator network [38]. The issue with standard CNNs or UNets is that they are not resolution-invariant (or do not treat images as functions). Therefore, we explore operator-valued NNs as our score functions. In our experiments, a novel trace class FNO-based latent distribution leads to SBDMs that yield reasonable quality images at a fixed resolution and generalize across resolutions, see [section 5](#). However, the FNO prior is unfortunately not strictly positive definite. Therefore, we propose a combined prior of FNO and Laplacian, which yields the best results. Our experiments show the need to change the latent distribution and the score network approximation.

Related work. Infinite-dimensional extensions of generative adversarial networks (GANs) have recently shown promise for generating function-valued data such as images. For example, GANOs [44] replace the latent distribution by Gaussian random fields and introduce a continuous loss. In [10] the infinite-dimensional representation of images is combined with an adversarial loss. Furthermore, [33] uses a layer-adding strategy to enable multilevel training. The recent paper [36] trains a diffusion model on a single image view a hierarchical ansatz, which generates first coarse and then finer images based on a single image. This is another way to achieve coarse-to-fine image generation.

The ideas in our paper most closely resemble the themes of the concurrent works [34, 39, 43, 13]. While [43] considers a Langevin SDE, we take a time schedule into account. Furthermore, our proof of the Wasserstein distance on the path measures uses some ideas in [43]. While their work is focused on defining the infinite-dimensional score object, we provide in-depth proofs of approximations on different levels and operate in finite dimensions to ensure the Lipschitz assumptions.

An infinite-dimensional extension of the DDPM framework [28] and promising results for

generating time series data is presented in [34]. In contrast to this work, we prefer the SBDM as it also leads to a continuous process in time. The infinite-dimensional SBDM frameworks in [13, 43, 39] and our approach model the generation problem in Hilbert spaces, employ trace class noise and contain similar theoretical results with some subtle differences. Similar to [39] we see benefits of approximating the score function with a Fourier neural operator network. Compared to [39], which solves the training problem in Hilbert space, we construct sequences of finite-dimensional approximations by solving suitable training problems in Euclidean space and show their convergence. The recent paper [13] considers a different kind of score model numerically, and they employ the notion of reverse solution of [41]. They show a sampling theorem, which discusses the condition that one can reconstruct an infinite-dimensional function from a countable set of points. Another recent work [5] uses the truncated Gaussian kernel and a U-Net-inspired multiscale architecture. It demonstrates good performance on super-resolution and inpainting problems.

What sets our work apart from the above papers is our focus on classical image generation problems, albeit with relatively simple datasets, and our emphasis on multilevel training. We provide the theoretical guarantee of the convergence of the discretization of the infinite-dimensional diffusion model and demonstrate the viability of multilevel training on the path of the forward SDE. We believe our paper is accessible to mathematicians and computer scientists without a background in stochastic analysis by giving detailed derivations and rigorous proofs. Moreover, we believe the experiment on different choices of prior distributions sheds some light on future improvements in infinite-dimensional diffusion models.

A multiscale diffusion approach based on Haar-Wavelets and non-uniform diffusion models is presented in [4]. This method uses different score models for each diffusion scale and anneals each pixel at a different speed. The numerical results suggest some advantages of exploiting different scales in terms of training time. While our multilevel approach considers a coarse-to-fine hierarchy of convergent discretizations and, importantly, we use a trace class operator to model the latent distributions and achieve a well-posed infinite-dimensional problem; see also discussion in [64]. A coarse-to-fine diffusion approach was also proposed in [46, 37] with different choices of the forward operator. A heat dissipation forward operator was presented in [46], whereas [37] suggested a blurring operator that diffuses different frequencies at different speeds. The idea of training at different resolutions without infinite-dimensional motivation has also been employed in [29]. A recent wave of infinite-dimensional generative models has also been applied to inverse problems, namely [1, 3].

The paper is organized as follows. In [section 2](#), we consider the finite-dimensional Euclidean setting and define an SBDM that maps the data distribution to a Gaussian with zero mean and general covariance matrix. Then, in the [section 3](#), we interpret and analyze the SBDM in the infinite-dimensional Hilbert space setting, present our discretization approach, and show their consistency. In [section 4](#), we demonstrate the design of diffusion models that enable the operations on function space, mainly in terms of the neural network architecture and the prior distribution of the forward SDEs. In [section 5](#), we provide experiments with different covariance operators, network architectures, and resolution scales using the MNIST and Fashion MNIST. Finally, in [section 6](#), we discuss our findings and identify open questions.

2. Finite-dimensional Score-Based Diffusion Models. Following the general steps of [30, 58, 56], we present the forward and reverse process of a score-based diffusion model that maps the data distribution \mathbb{P}_{data} to the latent distribution \mathbb{P}_Z on \mathbb{R}^d for some finite dimension d . Our presentation in subsection 2.1 lays the foundation for the infinite-dimensional case by generalizing the SBDM for Gaussians with general covariance matrices. In subsection 2.2, we show why the common choice of an identity covariance matrix and other covariance matrices whose trace grows in the dimension does not yield a well-posed infinite-dimensional limit.

2.1. Finite-dimensional Stochastic differential equations. The main idea of SBDMs consists of constructing a pair of stochastic differential equations, namely a forward and a reverse one, such that the forward process transforms the data into noise, and the reverse process transforms the noise into data.

The forward SDE computes a chain of random variables $X_t \in \mathbb{R}^d$, $t \in [0, T]$ by solving

$$(2.1) \quad dX_t = f(t, X_t) dt + g(t) dW_t^Q$$

with some initial condition $X_0 \sim \mathbb{P}_0 := \mathbb{P}_{\text{data}}$, noise process $W_t^Q = \sqrt{Q}W_t$, where W_t is a standard Brownian motion and $Q \in \mathbb{R}^{d \times d}$ is a symmetric positive definite covariance matrix, and, similar to [30, 58], we choose

$$(2.2) \quad f(t, X_t) := -\frac{1}{2}\alpha_t X_t, \quad g(t, X_t) = g(t) := \sqrt{\alpha_t}.$$

Here, $\alpha_t \in (0, \infty)$ is a positive and increasing schedule. With the above choices, the final distribution X_T is near $Y_0 \sim \mathbb{P}_Z$. By p_t we denote the density of $X_t \sim \mathbb{P}_{X_t}$ at $t \in [0, T]$ with respect to the Lebesgue measure. It is most common to use $Q = \text{Id}$ (the identity matrix on \mathbb{R}^d). However, we show that this choice is inadequate in the infinite-dimensional setting.

Under certain assumptions, cf. [2, 26], the reverse process $Y_t := X_{T-t}$ satisfies

$$(2.3) \quad dY_t = \left(-f(T-t, Y_t) + g(T-t)^2 Q \nabla \log p_{T-t}(Y_t)\right) dt + g(T-t) dW_t^Q,$$

which is, in contrast to the forward SDE, a nonlinear SDE whose drift depends on the gradient of the *score*, $\nabla \log p_t$, the log density of X_t . The reverse SDE can be derived from the standard SBDM used in [30, 58, 56] with the Brownian motion W_t^{Id} , by setting $g(t) := \sqrt{\alpha_t Q}$ in the standard SBDM.

To reverse the forward SDE, i.e., to go from the latent distribution $Y_0 \sim \mathbb{P}_Z$ to Y_T near \mathbb{P}_{data} , we need to learn the score of the forward process. In [28, 30, 58], it is proposed to approximate the score with the neural network $s_\theta(t, x(t))$ and train its weights by minimizing the expected least-square error between the output of the network and the true score via

$$\min_{\theta} \mathbb{E}_{t \sim U[0, T]} \mathbb{E}_{x(t) \sim \mathbb{P}_t} [\|s_\theta(t, x(t)) - Q \nabla \log p_t(x(t))\|^2].$$

Note that there are different ways to define this loss if $Q \neq \text{Id}$. For example, we could also optimize s_θ in such a way that $Q s_\theta(t, x(t)) \approx Q \nabla \log p_t(x(t))$. Since the score function cannot be observed in practice, [31, 63] showed that the above minimization problem is equivalent to $\min_{\theta} L_{\text{DSM}}(\theta)$ with

$$L_{\text{DSM}}(\theta) = \mathbb{E}_{x(0) \sim \mathbb{P}_{\text{data}}, t \sim U[0, T]} \mathbb{E}_{x(t) \sim \mathbb{P}_{X_t | X_0 = x(0)}} [\|s_\theta(t, x(t)) - Q \nabla \log p_t(x(t) | x(0))\|^2],$$

which does not involve the score $\nabla \log p_t$ itself, but instead the conditional distribution. In our case (2.2) the conditional distribution is Gaussian, i.e., $\mathbb{P}_{X_t|X_0=x(0)} = \mathcal{N}(\tilde{\alpha}_t x(0), \tilde{\beta}_t Q)$. where $\tilde{\alpha}_t = a_t^{-1}$, $\tilde{\beta}_t = (1 - \frac{1}{a_t^2})$, and $a_t = e^{\frac{1}{2} \int_0^t \alpha_r dr}$. This can be seen either by discretization [28] or by our [Theorem 3.1](#), which uses the variation of constants formula. This implies

$$(2.4) \quad \begin{aligned} \nabla \log p(x(t)|x(0)) &= \nabla \left(-\frac{1}{2} (x(t) - \tilde{\alpha}_t x(0))^T \tilde{\beta}_t^{-1} Q^{-1} (x(t) - \tilde{\alpha}_t x(0)) \right) \\ &= -\tilde{\beta}_t^{-1} Q^{-1} (x(t) - \tilde{\alpha}_t x(0)). \end{aligned}$$

Plugging this into the loss function, we get

$$(2.5) \quad L_{DSM}(\theta) = \mathbb{E}_{x(0) \sim \mathbb{P}_{\text{data}}, t \sim U[0, T]} \mathbb{E}_{x(t) \sim \mathbb{P}_{X_t|X_0=x(0)}} \left[\left\| s_\theta(t, x(t)) + \frac{x(t) - \tilde{\alpha}_t x(0)}{\tilde{\beta}_t} \right\|^2 \right].$$

Setting $\eta := \tilde{\beta}_t^{-1/2} (x(t) - \tilde{\alpha}_t x(0)) \sim \mathcal{N}(0, Q)$, this can be further simplified to

$$(2.6) \quad L_{DSM}(\theta) = \mathbb{E}_{x(0) \sim \mathbb{P}_{\text{data}}, t \sim U[0, T]} \mathbb{E}_{x(t) \sim \mathbb{P}_{X_t|X_0=x(0)}} \left[\left\| s_\theta(t, x(t)) + \tilde{\beta}_t^{-\frac{1}{2}} \eta \right\|^2 \right],$$

see also [58, 64]. Note that $\tilde{\beta}_t$ vanishes when t approaches 0. In the experiment, we consider the loss $\tilde{\beta}_t L_{DSM}(\theta)$ similar to [30].

Remark 2.1. When discretizing in time, the forward and reverse models become a pair of Markov chains. A rigorous framework of these schemes also in the case of non-absolutely continuous distributions and its relation to (stochastic) normalizing flow architectures was considered in [23, 24]. For a finite number of time steps, the DDPM framework [28, 55, 58] is recovered. In particular, these works minimize the joint Kullback–Leibler divergence between a forward path and the reverse path as a loss function.

2.2. Motivation for trace class Gaussian measures. We briefly discuss that the common choice of $Q = \text{Id}$, while leading to a well-defined SBDM problem in finite dimensions, is not suitable for the infinite-dimensional extension of SBDM. The key issue is that there is no standard Gaussian random variable in infinite dimensions. To see why, consider the Euclidean norm of the standard Gaussian random variable X^d in \mathbb{R}^d , then it holds that

$$(2.7) \quad \mathbb{E}[\|X^d\|_2^2] = \text{tr}(\text{Id}) = d,$$

see also [61]. In particular, for $d \rightarrow \infty$ as in the function space limit, we see that $\mathbb{E}[\|X^d\|_2^2] \rightarrow \infty$. This is one way to see why the standard Gaussian distribution becomes problematic in infinite dimensions; see, e.g., [25, 59] for in-depth discussions of this issue.

This motivates the use of so-called *trace class operators* in infinite dimensions, i.e., operators whose trace remains bounded as $d \rightarrow \infty$ [25, 59]. As can be seen in (2.7), if Q is not trace class, then the ℓ^2 -sum of the entries of X^d goes to ∞ as the resolution approaches ∞ .

3. Score-Based Diffusion Models on Infinite-Dimensional Hilbert Spaces. In this section, we consider the SBDM problem for H -valued random variables, where H is a separable Hilbert space. The necessary preliminaries on Gaussian distributions on H , trace class operators $Q \in L(H)$, and Q -Wiener processes are given in [Appendix A](#). One of the key ideas is to express the processes in terms of the spectral decomposition of Q . In [subsection 3.1](#), we deal with the solution of the forward process and its approximation by finite-dimensional discretizations using the truncated spectral decomposition of Q . We prove an explicit formula for the discretization error and show convergence. In [subsection 3.2](#), we derive reverse SDEs for the discretized forward process and prove Wasserstein error bounds between the learned approximations of the reverse process and the data distribution.

Note that in this section, we provide outlines of the proofs to streamline the discussion; for full detail, we provide references to the supplementary material.

3.1. Forward SDE and its Discretization. Let $(H, \|\cdot\|)$ be a real separable Hilbert space, $K(H)$ the space of compact operators on H , and $Q \in K(H)$ a trace class operator. By $H_Q := Q^{\frac{1}{2}}H$, we denote the Cameron-Martin space of Q and by $L_2(H_Q, H)$ the space of Hilbert-Schmidt operators from H_Q into H , see [Appendix A](#). For a terminal time $T > 0$, consider continuous drift and diffusion functions $f: [0, T] \times H \rightarrow H$ and $g: [0, T] \rightarrow L_2(H_Q, H)$, respectively. We need the notion of strong and weak solutions of SDEs. For a given random variable $X_0 \in H$ on some probability space $(\Omega, \mathcal{F}, \mathbb{P})$ and a Q -Wiener process W^Q on $(\Omega, \mathcal{F}, \mathbb{P})$ that is independent of X_0 , we call a random process $(X_t)_{t \in [0, T]}$ on a *strong solution* of [\(2.1\)](#) with initial condition X_0 , if $(X_t)_{t \in [0, T]}$ has continuous sample paths, satisfies \mathbb{P} -almost surely

$$(3.1) \quad X_t = X_0 + \int_0^t f(s, X_s) ds + \int_0^t g(s) dW_s^Q, \quad t \in [0, T]$$

and is adapted to the smallest complete filtration $\mathbb{F} = (\mathcal{F})_{t \geq 0}$ in which X_0 is \mathcal{F}_0 -measurable and W^Q is \mathbb{F} -adapted. It is easy to check that, due to the independence of X_0 and W^Q , the process W^Q is also a Q -Wiener process on the *filtered probability space* $(\Omega, \mathcal{F}, \mathbb{F}, \mathbb{P})$.

We call a triple $((\Omega, \mathcal{F}, \mathbb{F}, \mathbb{P}), (X_t)_{t \in [0, T]}, W^Q)$ a *weak solution* of [\(2.1\)](#) with initial condition \mathbb{P}_0 if $(\Omega, \mathcal{F}, \mathbb{F}, \mathbb{P})$ is a filtered probability space with normal filtration, W^Q is a Q -Wiener process on $(\Omega, \mathcal{F}, \mathbb{F}, \mathbb{P})$, and $(X_t)_{t \in [0, T]}$ is \mathbb{F} -adapted, satisfies $X_0 \sim \mathbb{P}_0$, has continuous sample paths, and fulfills \mathbb{P} -almost surely [\(3.1\)](#). Note that the filtered probability space and the driving Q -Wiener process are part of the notion of weak solutions and not chosen a priori as is in the case of strong solutions. Clearly, any strong solution corresponds to a weak solution. However, the reverse is not true ([\[52, Ex. 3.7\]](#)).

We define the forward process by choosing the schedule $\alpha \in \mathcal{C}^1([0, T]; \mathbb{R}_{>0})$, the drift $f(t, x) := \frac{1}{2}\alpha_t x$, the diffusion $g(t) := \sqrt{\alpha_t}$, i.e., $g(t): H_Q \rightarrow H$ with $y \mapsto \sqrt{\alpha_t}y$. Thus we have

$$(3.2) \quad dX_t = -\frac{1}{2}\alpha_t X_t dt + \sqrt{\alpha_t} dW_t^Q$$

with initial condition $X_0 \sim \mathbb{P}_{\text{data}}$, where \mathbb{P}_{data} is the data distribution. The following theorem establishes the existence of a unique strong solution of [\(3.2\)](#) and provides an explicit formula for this solution. The existence and uniqueness statements of the theorem are based on [\[17, Theorem 3.3\]](#), and the explicit formula can be derived by a variation of constants type argument. The full proof is given in [Appendix B.1](#).

Theorem 3.1 (Variation of constants formula). *Let $X_0 \in H$ be a random variable and let W^Q be a Q -Wiener process that is independent of X_0 . Then the SDE (3.2) has a unique strong solution $(X_t)_{t \in [0, T]}$, which is given \mathbb{P} -almost surely for all $t \in [0, T]$ by*

$$(3.3) \quad X_t = a_t^{-1} \left(X_0 + \int_0^t a_s \sqrt{\alpha_s} dW_s^Q \right), \quad a_t := e^{\frac{1}{2} \int_0^t \alpha_r dr}.$$

If $\mathbb{E} [\|X_0\|^2] < \infty$, then it holds $\mathbb{E} \left[\sup_{t \in [0, T]} \|X_t\|^2 \right] < \infty$. Let W^Q have the Karhunen–Loève decomposition (A.3). Then, for all $t \in [0, T]$, the stochastic integral

$$(3.4) \quad B_t := \int_0^t a_s \sqrt{\alpha_s} dW_s^Q = \sum_{k \in \mathbb{N}} \sqrt{\lambda_k} \left(\int_0^t a_s \sqrt{\alpha_s} d\beta_k(s) \right) e_k,$$

is a centered $(a_t^2 - 1)Q$ -Gaussian.

Next, we discretize the H -valued forward process defined by (3.2) by truncating the Karhunen–Loève decomposition (A.3) of W^Q . Restricting the forward SDE (3.2) onto $H_n := \text{span}\{e_1, \dots, e_n\}$ yields the SDE

$$(3.5) \quad dX_t^n = -\frac{1}{2} \alpha_t X_t^n dt + \sqrt{\alpha_t} dW_t^{Q_n},$$

with initial condition $X_0^n := \sum_{k=1}^n \langle X_0, e_k \rangle e_k$ and

$$(3.6) \quad W_t^{Q_n} := \sum_{k=1}^n \sqrt{\lambda_k} \beta_k(t) e_k.$$

Setting $Q_n := \sum_{k=1}^n \lambda_k \langle e_k, \cdot \rangle e_k$, we note that W^{Q_n} is a Q_n -Wiener process, which justifies the notation. By Theorem 3.1, the restricted equation (3.5) has a unique strong solution that satisfies \mathbb{P} -almost surely

$$(3.7) \quad X_t^n = a_t^{-1} (X_0^n + B_t^n), \quad B_t^n := \int_0^t a_s \sqrt{\alpha_s} dW_s^{Q_n} = \sum_{k=1}^n \sqrt{\lambda_k} \int_0^t a_s \sqrt{\alpha_s} d\beta_k(s) e_k.$$

Since X_t^n is simply the projection of X_t onto H_n , we expect that it is a good approximation of X_t for large n . The next theorem gives an explicit bound on the approximation error and is similar to the argument in [43, Theorem 1].

Theorem 3.2 (Convergence of forward process). *Let W^Q be a Q -Wiener process with trace class operator Q having the Karhunen–Loève decomposition (A.3) and let W^{Q_n} be its truncation (3.6). If $(X_t)_{t \in [0, T]}$ denotes the solution of the SDE (3.2) and $(X_t^n)_{t \in [0, T]}$ the solution of the approximate problem (3.5), then*

$$(3.8) \quad \mathbb{E} [\|X_t - X_t^n\|^2] \leq 2 a_t^{-2} \mathbb{E} [\|X_0 - X_0^n\|^2] + 2(1 - a_t^{-2}) \text{tr}(Q - Q_n), \quad t \in [0, T],$$

and

$$\mathbb{E} \left[\sup_{t \in [0, T]} \|X_t - X_t^n\|^2 \right] \leq 2 \mathbb{E} [\|X_0 - X_0^n\|^2] + 8(a_T^2 - 1) \text{tr}(Q - Q_n).$$

If $X_0 \in H$ fulfills $\mathbb{E} [\|X_0\|^2] < \infty$, then $\mathbb{E} \left[\sup_{t \in [0, T]} \|X_t - X_t^n\|^2 \right] \rightarrow 0$ as $n \rightarrow \infty$.

Proof. By applying [Theorem 3.1](#) to the initial value $X_0 - X_0^n$ and the $(Q - Q_n)$ -Wiener process $W^Q - W^{Q_n}$, we obtain that

$$\delta B_t^n := \int_0^t a_s \sqrt{\alpha_s} d(W_s^Q - W_s^{Q_n})$$

is a centered $(a_t^2 - 1)(Q - Q_n)$ -Gaussian and

$$\mathbb{E} \left[\|\delta B_t^n\|^2 \right] = (a_t^2 - 1) \operatorname{tr}(Q - Q_n).$$

Utilizing the variation of constants formula [\(3.3\)](#), we conclude

$$\begin{aligned} (3.9) \quad X_t - X_t^n &= a_t^{-1} \left(X_0 - X_0^n + \int_0^t a_s \sqrt{\alpha_s} dW_s^Q - \int_0^t a_s \sqrt{\alpha_s} dW_s^{Q_n} \right) \\ &= a_t^{-1} \left(X_0 - X_0^n + \delta B_t^n \right). \end{aligned}$$

In summary, we get

$$\begin{aligned} (3.10) \quad \mathbb{E} \left[\|X_t - X_t^n\|^2 \right] &\leq 2 a_t^{-2} \mathbb{E} \left[\|X_0 - X_0^n\|^2 \right] + 2 a_t^{-2} \mathbb{E} \left[\|\delta B_t^n\|^2 \right] \\ &\leq 2 a_t^{-2} \mathbb{E} \left[\|X_0 - X_0^n\|^2 \right] + 2 (1 - a_t^{-2}) \operatorname{tr}(Q - Q_n), \end{aligned}$$

which proves [\(3.8\)](#). Furthermore, since δB_t^n is a square-integrable martingale, Doob's maximal inequality [\[17, Thm 2.2\]](#) yields

$$\mathbb{E} \left[\sup_{t \in [0, T]} \|\delta B_t^n\|^2 \right] \leq 4 \mathbb{E} \left[\|\delta B_T^n\|^2 \right] = 4 (a_T^2 - 1) \operatorname{tr}(Q - Q_n).$$

This proves

$$\mathbb{E} \left[\sup_{t \in [0, T]} \|X_t - X_t^n\|^2 \right] \leq 2 \mathbb{E} \left[\|X_0 - X_0^n\|^2 \right] + 8 (a_T^2 - 1) \operatorname{tr}(Q - Q_n).$$

For any $\omega \in \Omega$, we have $\|X_0(\omega) - X_0^n(\omega)\|^2 = \sum_{k=n+1}^{\infty} |\langle X_0(\omega), e_k \rangle|^2$ which goes to zero. Thus, the assertion follows by dominated convergence since $\mathbb{E} \left[\|X_0\|^2 \right] < \infty$. ■

Next, we estimate the approximation error with respect to the Wasserstein-2 distance [\[62, Def 6.1\]](#) that for two measures μ, ν on a separable metric space (K, d) is defined by

$$W_2(\mu, \nu) := \left(\min_{\pi \in \Pi(\mu, \nu)} \int d(x, y)^2 d\pi(x, y) \right)^{1/2} = \left(\min_{X \sim \mu, Y \sim \nu} \mathbb{E}(d(X, Y)^2) \right)^{1/2},$$

where $\Pi(\mu, \nu)$ denotes the set of measures on $K \times K$ with marginals μ and ν , i.e. $\pi(B \times K) = \mu(B)$, $\pi(K \times B) = \nu(B)$ for all $B \in \mathcal{B}(K)$, where $\mathcal{B}(K)$ is the Borel σ -algebra of K . The Wasserstein-2 distance is a metric on the space of probability measures on K having finite second moments. The following corollary, which is an immediate consequence of [Theorem 3.2](#), establishes convergence of the forward process with respect to the Wasserstein-2 distance.

Corollary 3.3. *Let $X_0 \in H$ be a random variable fulfilling $\mathbb{E} [\|X_0\|^2] < \infty$. Let $(X_t)_{t \in [0, T]}$ denote the solution of the SDE (3.2) and $(X_t^n)_{t \in [0, T]}$ the solution of the approximate problem (3.5) with corresponding laws \mathbb{P}_{X_t} and $\mathbb{P}_{X_t^n}$. Then it holds for $t \in [0, T]$ that*

$$W_2^2(\mathbb{P}_{X_t^n}, \mathbb{P}_{X_t}) \leq 2a_t^{-2} \mathbb{E} [\|X_0 - X_0^n\|^2] + 2(1 - a_t^{-2}) \operatorname{tr}(Q - Q_n) \rightarrow 0 \text{ as } n \rightarrow \infty.$$

3.2. Reverse Process. In the finite-dimensional setting, the reverse process $Y_t := X_{T-t}$, $t \in [0, T]$, is the solution of a reverse SDE whose drift depends on the score function; see our discussion in section 2. This score is defined via the Lebesgue density of the finite-dimensional forward process. Since Lebesgue densities no longer exist in the infinite-dimensional Hilbert space setting, the definition of the score is not straightforward. Some results on time reversibility of infinite-dimensional diffusion processes are discussed in [15, 41, 43].

In this paper, we circumvent the issue of time-reversal of the infinite-dimensional forward process by discretizing the forward process and working only with time-reversals of the discretizations. As discussed in section 2, the time reversal of a diffusion process in \mathbb{R}^n is well understood. Thus, it is natural to relate the discretized forward SDE (3.5) to an equivalent SDE in \mathbb{R}^n via coordinate-vectors and then transfer the reverse SDE in \mathbb{R}^n back to an SDE in H_n . To this end, we define for $n \in \mathbb{N}$, the isometric isomorphism

$$\iota_n: H_n \rightarrow \mathbb{R}^n, \quad \iota_n(x) := (\langle x, e_k \rangle)_{k=1}^n.$$

Using the coordinate process $\hat{X}_t^n := \iota_n(X_t^n)$, we can formulate a reverse SDE to the restricted forward SDE (3.5) under mild assumptions.

Theorem 3.4 (Discretized reverse process). *Let W^Q be a Q -Wiener process with injective trace class operator Q having the Karhunen–Loève decomposition (A.3), and let W^{Q_n} be its truncation (3.6). Let X_t^n be the solution of the approximate problem (3.5). If the random variable $\hat{X}_0^n \in \mathbb{R}^n$ admits a Lebesgue density p_0^n , then $\hat{X}_t^n \in \mathbb{R}^n$ admits a Lebesgue density p_t^n and it holds for $t \in (0, T]$ that*

$$(3.11) \quad \nabla \log p_t^n(z) = -\frac{a_t}{(a_t^2 - 1)} \left(\frac{(\lambda_k)^{-1} (p_0^n * (z_k b_t^n)) (a_t z)}{(p_0^n * b_t^n)(a_t z)} \right)_{k=1}^n,$$

where $*$ denotes the convolution and

$$(3.12) \quad b_t^n(z) := e^{-\frac{(a_t^2 - 1)^{-1}}{2} z^\top \operatorname{diag}(\lambda_1, \dots, \lambda_n)^{-1} z}, \quad t \in (0, T].$$

In particular, the discretized score

$$(3.13) \quad f^n(t, \cdot) := \alpha_{T-t} Q_n (\iota_n^{-1} \circ \nabla \log p_{T-t}^n \circ \iota_n), \quad t \in [0, T),$$

is well-defined, and Lipschitz continuous in the second variable uniformly on $[0, T - \delta] \times \{x \in H_n \mid \|x\| \leq N\}$ for all $\delta > 0$ and $N \in \mathbb{N}$. The discretized reverse SDE

$$(3.14) \quad dY_t^n = \left(\frac{1}{2} \alpha_{T-t} Y_t^n + f^n(t, Y_t^n) \right) dt + \sqrt{\alpha_{T-t}} d\hat{W}_t^{Q_n},$$

with initial condition $Y_0^n \sim \mathbb{P}_{X_T^n}$ admits a weak solution $((\hat{\Omega}, \hat{\mathcal{F}}, \hat{\mathbb{F}}, \hat{\mathbb{P}}), (Y_t^n)_{t \in [0, T]}, \hat{W}^{Q_n})$ such that $(Y_t^n)_{t \in [0, T]}$ is equal to $(X_{T-t}^n)_{t \in [0, T]}$ in distribution. $(\hat{\Omega}, \hat{\mathcal{F}}, \hat{\mathbb{F}}, \hat{\mathbb{P}})$ can be chosen as an extension of $(\Omega, \mathcal{F}, \mathbb{F}, \mathbb{P})$, where \mathbb{F} denotes the completion of the natural filtration of $(X_{T-t}^n)_{t \in [0, T]}$, and $(Y_t^n)_{t \in [0, T]}$ as the canonical extension of $(X_{T-t}^n)_{t \in [0, T]}$ to this extended probability space, cf. [52, Def. 3.13]. Furthermore, solutions of (3.14) are unique in law, i.e., any weak solution with initial distribution $\mathbb{P}_{X_T^n}$ is equal to $(X_{T-t}^n)_{t \in [0, T]}$ in distribution.

The following proof contains the main ideas. For convenience, we have further detailed some parts in an extended proof in the [Appendix B.2](#).

Proof. 1. First, we show that p_t^n has the form (3.11) which then implies that f^n in (3.13) is well-defined with the desired properties. We first check that \hat{X}_t^n has the density

$$p_t^n(z) := \frac{a_t^n (\lambda_1 \dots \lambda_n)^{-1/2}}{(2\pi(a_t^2 - 1))^{n/2}} (p_0^n * b_t^n)(a_t z).$$

Then, using regularity properties, we conclude that f^n as in (3.13) is well-defined and Lipschitz continuous in the second variable uniformly on $[0, T - \delta] \times \{x \in H_n \mid \|x\| \leq N\}$.

2. Next, we transfer (3.5) to an SDE on \mathbb{R}^n to obtain a reverse equation. Let $\beta_k(t)$, $k \in \mathbb{N}$ be as in (A.3). Then $\beta_t^n := (\beta_k(t))_{k=1}^n$ is an n -dimensional Brownian motion and $(\hat{X}_t^n)_{t \in [0, T]}$ is the unique strong solution of $d\hat{X}_t^n = -\frac{1}{2}\alpha_t \hat{X}_t^n dt + \sqrt{\alpha_t} \text{diag}(\sqrt{\lambda_1}, \dots, \sqrt{\lambda_n}) d\beta_t^n$ with initial value \hat{X}_0^n . We set $\Lambda = \text{diag}(\lambda_1, \dots, \lambda_n)$. We conclude that $(\hat{X}_{T-t}^n)_{t \in [0, T]}$ is a weak solution of

$$(3.15) \quad d\hat{Y}_t^n = \left(\frac{1}{2}\alpha_{T-t} \hat{Y}_t^n + \alpha_{T-t} \Lambda \nabla \log p_{T-t}^n(\hat{Y}_t^n) \right) dt + \sqrt{\alpha_{T-t}} \sqrt{\Lambda} d\hat{\beta}_t^n$$

with initial condition $\hat{Y}_0^n \sim \mathbb{P}_{\hat{X}_T^n}$, by [26, Thm 2.1]. Thus, $(\hat{Y}_t^n)_{t \in [0, T]}$ is equal to $(\hat{X}_{T-t}^n)_{t \in [0, T]}$ in distribution. We set $Y_t^n := \iota_n^{-1}(\hat{Y}_t^n)$. Clearly, $(Y_t^n)_{t \in [0, T]}$ and $(X_{T-t}^n)_{t \in [0, T]}$ are equal in distribution. Since $((\hat{\Omega}, \hat{\mathcal{F}}, \hat{\mathbb{F}}, \hat{\mathbb{P}}), (\hat{Y}_t^n)_{t \in [0, T]}, \hat{\beta}^n)$ is a weak solution of (3.15), the process $(Y_t^n)_{t \in [0, T]}$ has continuous sample-paths and is adapted to $\hat{\mathbb{F}}$. Further, since Y_t^n fulfills (3.1) for the setting (3.15), we have $\hat{\mathbb{P}}$ -almost surely for all $t \in [0, T]$ that Y_t^n is equal to

$$Y_0^n + \int_0^t \frac{1}{2} \alpha_{T-s} Y_s^n + \underbrace{\alpha_{T-s} Q_n(\iota_n^{-1} \circ \nabla \log p_{T-t}^n \circ \iota_n)(Y_s^n)}_{=f^n(s, Y_s^n)} ds + \int_0^t \sqrt{\alpha_{T-s}} d\hat{W}_s^{Q_n}$$

Thus $((\hat{\Omega}, \hat{\mathcal{F}}, \hat{\mathbb{F}}, \hat{\mathbb{P}}), (Y_t^n)_{t \in [0, T]}, \hat{W}^{Q_n})$ is a weak solution of (3.14) with $Y_0^n \sim \mathbb{P}_{X_T^n}$.

We can analogously show that $((\hat{\Omega}, \hat{\mathcal{F}}, \hat{\mathbb{F}}, \hat{\mathbb{P}}), (\hat{Y}_t^n)_{t \in [0, T]}, \hat{\beta}^n)$ with $\hat{Y}_t^n := \iota_n(Y_t^n)$ and $\hat{\beta}_t^n := ((\sqrt{\lambda_k})^{-1} \langle \hat{W}_t^{Q_n}, e_k \rangle)_{k=1}^n$ yields a weak solution of (3.15). Thus, showing uniqueness in law of (3.15) is sufficient to prove uniqueness in law of (3.14). Since the drift and diffusion coefficients of (3.15) are Lipschitz continuous in the second variable on sets of the form $[0, T - \delta] \times \{z \in \mathbb{R}^n \mid \|z\| \leq N\}$, we know by [49, Lem. 12.4] and [49, Definition 12.1] that pathwise uniqueness holds on $[0, T - \delta]$. A limiting argument $\delta \rightarrow 0$ yields pathwise uniqueness on $[0, T]$. \blacksquare

As a consequence of the theorem, we obtain the following corollary.

Corollary 3.5. *Let $X_0 \in H$ be a random variable fulfilling $\mathbb{E}[\|X_0\|^2] < \infty$. Further, let X_t^n be the solution of the approximate problem (3.5), and let $\hat{X}_0^n \in \mathbb{R}^n$ admit a Lebesgue density. Then we have for $t \in [0, T)$ that*

$$W_2^2(\mathbb{P}_{Y_t^n}, \mathbb{P}_{X_{T-t}^n}) \leq 2a_{T-t}^{-2} \mathbb{E}[\|X_0 - X_0^n\|^2] + 2(1 - a_{T-t}^{-2}) \text{tr}(Q - Q_n) \rightarrow 0 \text{ as } n \rightarrow \infty.$$

Proof. The assertion follows from the triangle inequality

$$W_2(\mathbb{P}_{Y_t^n}, \mathbb{P}_{X_{T-t}^n}) \leq W_2(\mathbb{P}_{Y_t^n}, \mathbb{P}_{X_{T-t}^n}) + W_2(\mathbb{P}_{X_{T-t}^n}, \mathbb{P}_{X_{T-t}^n})$$

Theorem 3.4 and **Corollary 3.3.** ■

Besides the discretized reverse SDE (3.14), we also consider the case of approximation errors in the reverse drift, i.e.,

$$(3.16) \quad d\tilde{Y}_t^n = \left(\frac{1}{2} \alpha_{T-t} \tilde{Y}_t^n + \tilde{f}^n(t, \tilde{Y}_t^n) \right) dt + \sqrt{\alpha_{T-t}} d\hat{W}_t^{Q_n},$$

where \tilde{f}^n could be a neural network, which is learned via the DSM loss, that is supposed to approximate the forward path score $f^n(t, X_{T-t}^n)$ in (3.13). In contrast to the discretized reverse SDE, the approximate reverse SDE is started at the latent distribution $\tilde{Y}_0^n \sim \mathcal{N}(0, Q_n)$.

We now prove that when the denoising score matching loss in (2.6) decreases, the distribution of the approximated reverse equation also goes to the distribution of the time-changed forward process. Similar to [43, Theorem 2], we bound the *Wasserstein distance between path measures obtained by our SDE*. However, we include a time schedule, consider the finite-dimensional case, and explicitly bound the distance for all intermediate times. More precisely, we consider a path $Z = (Z_t)_{t \in [0, t_0]}$ as a $\mathcal{C}([0, t_0], H)$ -valued random variable on $(\Omega, \mathcal{F}, \mathbb{P})$ with

$$\|Z\|_{L^2(\Omega, \mathcal{F}, \mathbb{P}; \mathcal{C}([0, t_0], H))}^2 := \mathbb{E} \left[\sup_{t \in [0, t_0]} \|Z_t\|^2 \right].$$

Then we can examine the Wasserstein distance of two path measures of the form $\mathbb{P}_{(Z_t)_{t \in [0, t_0]}}$ by noting that the space $\mathcal{C}([0, t_0], H)$ equipped with the uniform norm is a separable metric space. For notational simplicity, we denote a path measure $\mathbb{P}_{(Z_t)_{t \in [0, t_0]}}$ by $\mathbb{P}_{(Z_t)_{t_0}}$. The proof combines classical concepts in stochastic analysis such as, e.g., Gronwall's lemma and Jensen's inequality, as well as results from [53, Thm 18.11], [9, Prop. 7.18], [6, Thm 1.2], and [32, Prop. C.1]. We give a streamlined version of the proof and refer to [Appendix B.3](#) for details.

Theorem 3.6. *Let $X_0 \in H$ be a random variable fulfilling $\mathbb{E}[\|X_0\|^2] < \infty$ and let Q be an injective trace class operator on H . For $n \in \mathbb{N}$, let $(X_t^n)_{t \in [0, T]}$ denote the solution of the approximate problem (3.5) and let $\hat{X}_0^n \in \mathbb{R}^n$ admit a Lebesgue density. For $t_0 < T$, assume that for any $s \in [0, t_0]$ the approximated score \tilde{f}^n restricted to $[0, s] \times H_n$ is continuous and Lipschitz continuous in the second variable with Lipschitz constant L_s^n and that*

$$(3.17) \quad \mathbb{E} \left[\int_0^{t_0} \|f^n(s, X_{T-s}^n) - \tilde{f}^n(s, X_{T-s}^n)\|^2 ds \right] \leq \varepsilon$$

is satisfied. By $\mathbb{P}(\tilde{Y}_t^n)_{t_0}$ denote the path measure induced by (3.16) with initial distribution $\mathcal{N}(0, Q_n)$. Then it holds

$$(3.18) \quad W_2^2(\mathbb{P}(X_{T-t}^n)_{t_0}, \mathbb{P}(\tilde{Y}_t^n)_{t_0}) \leq 12 \left(t_0 \varepsilon e^{4\xi(t_0)t_0^2} + e^{3\xi(t_0)t_0^2} W_2^2(\mathbb{P}_{X_T^n}, \mathcal{N}(0, Q_n)) \right),$$

where $\xi(t_0) := \sup_{s \in [0, t_0]} \left(\frac{\alpha_{T-s}^2}{4} + (L_s^n)^2 \right)$.

Proof. 1. First, we conclude by Lipschitz continuity of \tilde{f}^n , for any initial condition and Q_n -Wiener process independent of the initial condition the SDE (3.16) has a unique strong solution on $[0, t_0]$. We use $\mathbb{P}(\check{Y}_t^n)_{t_0}$ to denote the path measure induced by (3.16), but with initial distribution $\mathbb{P}_{X_T^n}$. By the triangle inequality, we obtain

$$(3.19) \quad W_2^2(\mathbb{P}(X_{T-t}^n)_{t_0}, \mathbb{P}(\tilde{Y}_t^n)_{t_0}) \leq 4W_2^2(\mathbb{P}(X_{T-t}^n)_{t_0}, \mathbb{P}(Y_t^n)_{t_0}) \\ + 2W_2^2(\mathbb{P}(Y_t^n)_{t_0}, \mathbb{P}(\check{Y}_t^n)_{t_0}) + 4W_2^2(\mathbb{P}(\check{Y}_t^n)_{t_0}, \mathbb{P}(\tilde{Y}_t^n)_{t_0}).$$

By Theorem 3.4, the first term is zero.

2. Next, we bound the third term. Let \check{Y}_0^n and \tilde{Y}_0^n be any realizations of $\mathbb{P}_{X_T^n}$ and $\mathcal{N}(0, Q_n)$, respectively, that are defined on the same probability space. For some driving Q_n -Wiener process independent of \check{Y}_0^n and \tilde{Y}_0^n and defined on the same probability space (or possibly an extension of it), let $(\check{Y}_t^n)_{t \in [0, t_0]}$ and $(\tilde{Y}_t^n)_{t \in [0, t_0]}$ be the unique strong solutions of (3.16) started from \check{Y}_0^n and \tilde{Y}_0^n , respectively. By (3.1) and using Jensen's inequality, we obtain for $s \in [0, t_0]$,

$$(3.20) \quad \|\check{Y}_s^n - \tilde{Y}_s^n\|^2 \leq 3 \left(\|\check{Y}_0^n - \tilde{Y}_0^n\|^2 + \left\| \int_0^s \frac{1}{2} \alpha_{T-r} (\check{Y}_r^n - \tilde{Y}_r^n) dr \right\|^2 \right) \\ + \left\| \int_0^s \tilde{f}^n(r, \check{Y}_r^n) - \tilde{f}^n(r, \tilde{Y}_r^n) dr \right\|^2 \\ \leq 3 \|\check{Y}_0^n - \tilde{Y}_0^n\|^2 + 3t_0 \sup_{r \in [0, t_0]} \left(\frac{\alpha_{T-r}^2}{4} + (L_r^n)^2 \right) \int_0^s \|\check{Y}_r^n - \tilde{Y}_r^n\|^2 dr.$$

Setting $h_1(t) := \mathbb{E}[\sup_{s \in [0, t]} \|\check{Y}_s^n - \tilde{Y}_s^n\|^2]$ for $t \in [0, t_0]$, we consequently obtain

$$(3.21) \quad h_1(t) \leq 3\mathbb{E}[\|\check{Y}_0^n - \tilde{Y}_0^n\|^2] + 3t_0\xi(t_0) \int_0^t h_1(r) dr,$$

by Fubini's theorem. By Theorem 3.1, $\mathbb{E}[\sup_{t \in [T-t_0, T]} \|X_t^n\|^2] < \infty$. In particular, $\mathbb{E}[\|\check{Y}_0^n\|^2] = \mathbb{E}[\|X_T^n\|^2] < \infty$. $\mathbb{E}[\|\tilde{Y}_0^n\|^2] = \text{tr}(Q_n) < \infty$. Since $h_1 \in L^\infty([0, t_0])$, we apply Gronwall's lemma to h_1 and obtain for all $t \in [0, t_0]$ that

$$h_1(t) \leq 3\mathbb{E}[\|\check{Y}_0^n - \tilde{Y}_0^n\|^2] e^{3\xi(t_0)t_0 t}.$$

In particular, the Wasserstein-2 distance can be estimated by

$$(3.22) \quad W_2^2(\mathbb{P}(\check{Y}_t^n)_{t_0}, \mathbb{P}(\tilde{Y}_t^n)_{t_0}) \leq \mathbb{E} \left[\sup_{s \in [0, t_0]} \|\check{Y}_s^n - \tilde{Y}_s^n\|^2 \right] = h_1(t_0) \\ = 3 e^{3\xi(t_0)t_0^2} W_2^2(\mathbb{P}_{X_T^n}, \mathcal{N}(0, Q_n)),$$

where we used that the previous estimates are valid for an arbitrary realization of \check{Y}_0^n and \tilde{Y}_0^n .
3. We define $(\check{Y}_t^n)_{t \in [0, t_0]}$ as the strong solution of the approximate reverse (3.16) with the initial condition $\check{Y}_0^n = Y_0^n$ and the same driving noise \hat{W}^{Q^n} . As before, we can bound the difference as follows for $s \in [0, t_0]$:

$$(3.23) \quad \begin{aligned} \|Y_s^n - \check{Y}_s^n\|^2 &\leq \left\| Y_0^n - \check{Y}_0^n + \int_0^s \frac{1}{2} \alpha_{T-r} (Y_r^n - \check{Y}_r^n) dr + \int_0^s f^n(r, Y_r^n) - \tilde{f}^n(r, \check{Y}_r^n) dr \right\|^2 \\ &\leq 2t_0 \sup_{r \in [0, t_0]} \frac{\alpha_{T-r}^2}{4} \int_0^s \|Y_r^n - \check{Y}_r^n\|^2 dr + 2t_0 \int_0^s \|f^n(r, Y_r^n) - \tilde{f}^n(r, \check{Y}_r^n)\|^2 dr. \end{aligned}$$

For the second term, we apply again the triangle inequality and obtain

$$(3.24) \quad \|f^n(r, Y_r^n) - \tilde{f}^n(r, \check{Y}_r^n)\|^2 \leq 2\|f^n(r, Y_r^n) - \tilde{f}^n(r, Y_r^n)\|^2 + 2 \sup_{r \in [0, t_0]} (L_r^n)^2 \|Y_r^n - \check{Y}_r^n\|^2.$$

Since $(Y_t^n)_{t \in [0, t_0]}$ is an extension of $(X_{T-t}^n)_{t \in [0, t_0]}$, we obtain from assumption (3.17) that

$$(3.25) \quad \mathbb{E} \left[\sup_{t \in [0, s]} \int_0^s \|f^n(r, Y_r^n) - \tilde{f}^n(r, Y_r^n)\|^2 dr \right] \leq \mathbb{E} \left[\int_0^{t_0} \|f^n(r, Y_r^n) - \tilde{f}^n(r, Y_r^n)\|^2 dr \right] \leq \varepsilon.$$

We set $h_2(t) := \mathbb{E}[\sup_{s \in [0, t]} \|Y_s^n - \check{Y}_s^n\|^2]$ for $t \in [0, t_0]$ and by Gronwall's lemma, it yields

$$(3.26) \quad W_2^2(\mathbb{P}^{(Y_t^n)_{t_0}}, \mathbb{P}^{(\check{Y}_t^n)_{t_0}}) \leq h_2(t_0) \leq 4t_0 \varepsilon e^{4\xi(t_0)t_0^2}.$$

In summary, we obtain (3.18). ■

Note that in the proof of [Theorem 3.6](#) we use the assumption that \hat{X}_0^n admits a Lebesgue density p_0^n only to apply [Theorem 3.4](#) and thus establish the existence of a weak solution of the discretized reverse SDE (3.14) that is equal to the time changed discretized forward process in distribution as well as uniqueness in law of solutions of (3.14). In [Theorem 3.4](#), the assumption that \hat{X}_0^n admits a Lebesgue density can be relaxed to \hat{X}_t^n admitting a Lebesgue density p_t^n for all times $t > 0$ such that (B.7) is satisfied and $\nabla \log p_t^n$ is well-defined and Lipschitz continuous in the second variable uniformly on $[\delta, T] \times \{z \in \mathbb{R}^n \mid \|z\| \leq N\}$ for all $\delta > 0$ and $N \in \mathbb{N}$. This weaker assumption can be met even if the data distribution is degenerate, as is illustrated in the following example where we consider Gaussian data distributions, which can be degenerate.

Our approximation result in [Theorem 3.6](#) requires bounded Lipschitz constants of the score for fixed $n \in \mathbb{N}$. To enable multilevel training, we do not want the sequence of Lipschitz constants to explode if $n \rightarrow \infty$. To this end, we consider the following example.

Example 3.7. *We consider a Gaussian data distribution, i.e., $\mathbb{P}_{\text{data}} = \mathcal{N}(\mu, P)$. We assume that Q is injective. Then the processes \hat{B}_t^n and \hat{X}_0^n are independent Gaussians.*

$$(3.27) \quad \begin{aligned} \hat{B}_t^n &\sim \mathcal{N}(0, (a_t^2 - 1) \hat{Q}_n) \text{ with } \hat{Q}_n := \text{diag}(\lambda_1, \dots, \lambda_n) \text{ and} \\ \hat{X}_0^n &\sim \mathcal{N}(\hat{\mu}^n, \hat{P}^n) \text{ with } \hat{\mu}^n := \iota_n \left(\sum_{k=1}^n \langle \mu, e_k \rangle e_k \right) \text{ and } \hat{P}^n := (\langle P e_i, e_j \rangle)_{i,j=1}^n, \end{aligned}$$

By (3.7) we have $\hat{X}_t^n = a_t^{-1} (\hat{X}_0^n + \hat{B}_t^n)$ and therefore $\hat{X}_t^n = \mathcal{N}(a_t^{-1} \hat{\mu}^n, a_t^{-2} \hat{P}_n + (1 - a_t^{-2}) \hat{Q}_n)$. In particular, the coordinate process \hat{X}_t^n has a density p_t^n for $t \in (0, T]$ that satisfies

$$(3.28) \quad \hat{Q}_n \nabla \log p_t^n(z) = -(1 - a_t^{-2})^{-1} \hat{Q}_n \left(\frac{a_t^{-2}}{1 - a_t^{-2}} \hat{P}_n + \hat{Q}_n \right)^{-1} (z - a_t^{-1} \hat{\mu}^n).$$

We assume that the spectral norms of $A_n := \hat{Q}_n \left(\frac{a_t^{-2}}{1 - a_t^{-2}} \hat{P}_n + \hat{Q}_n \right)^{-1}$ are uniformly bounded in n by some constant $C > 0$. This is equivalent to the condition that the smallest eigenvalues of

$$(3.29) \quad (A_n^T A_n)^{-1} := \hat{Q}_n^{-1} \left(\frac{a_t^{-2}}{1 - a_t^{-2}} \hat{P}_n + \hat{Q}_n \right)^2 \hat{Q}_n^{-1}$$

are bounded from below by C^{-2} . Note that while the eigenvalues of A_n^{-1} coincide with those of $\left(\frac{a_t^{-2}}{1 - a_t^{-2}} \hat{Q}_n^{-1/2} \hat{P}_n \hat{Q}_n^{-1/2} + I_n \right)$ and are therefore larger or equal than one, this is not necessarily longer true for $(A_n^T A_n)^{-1}$. However, the condition on (3.29) is always satisfied if \hat{P}_n is diagonal and can additionally be fulfilled by certain other matrices. Then we have for fixed $t_0 < T$ that

$$L_{t_0}^n := \sup_{t \in [T-t_0, T]} \left\| -\alpha_t (1 - a_t^{-2})^{-1} \hat{Q}_n \left(\frac{a_t^{-2}}{1 - a_t^{-2}} \hat{P}_n + \hat{Q}_n \right)^{-1} \right\| \leq \frac{C \sup_{t \in [T-t_0, T]} \alpha_t}{1 - e^{-\int_0^{T-t_0} \alpha_r dr}},$$

where $\|\cdot\|$ denotes the spectral norm on $\mathbb{R}^{n,n}$. In particular,

$$f^n(t, y) = \alpha_{T-t} Q_n (\iota_n^{-1} \circ \nabla \log p_{T-t}^n \circ \iota_n)(y) = \alpha_{T-t} \hat{Q}_n \nabla \log p_{T-t}^n(\iota_n(y))$$

is Lipschitz continuous in the second variable uniformly on $[0, t_0] \times H_n$ with the Lipschitz constant $L_{t_0}^n$ bounded independently of n for any $t_0 \in [0, T]$.

The next theorem shows the viability of multilevel training under the assumption that the score path random variable $f^n(t, X_{T-t}^n)$ converges. Under this assumption, one can bound the error (3.17) at level $m \geq n$ for the choice $\tilde{f}^m := \tilde{f}^n$. The $L^2(\Omega, \mathcal{F}, \mathbb{P}; L^2([0, t_0]; H))$ distance between the approximate score path $\tilde{f}^n(t, X_{T-t}^n)$ and the true one $f^m(t, X_{T-t}^m)$ can be bounded by the error (3.17) at level n plus some null sequence in n . Therefore, when choosing the level large enough, the learned score provides a good approximation for higher levels. However, these results only hold true on the path of the forward SDE.

Theorem 3.8. *Assume, for $t_0 < T$, that $F_t^n := f^n(t, X_{T-t}^n)$ converges to some process F_t with $F_t \in L^2(\Omega, \mathcal{F}, \mathbb{P}; L^2([0, t_0]; H))$. Further, let \tilde{f}^n be Lipschitz continuous with respect to the second component on $[0, t_0] \times H$ with Lipschitz constant $L_{t_0}^n$ bounded uniformly in n . Then, we have for $m \geq n$ and $\tilde{F}_t^{n,m} := \tilde{f}^n(t, X_{T-t}^m)$ that*

$$\mathbb{E} \left[\int_0^{t_0} \|\tilde{F}_t^{n,m} - F_t^m\|^2 dt \right] \leq 3 \mathbb{E} \left[\int_0^{t_0} \|\tilde{F}_t^{n,n} - F_t^n\|^2 dt \right] + \varepsilon_n,$$

where $\varepsilon_n \rightarrow 0$ as $n \rightarrow \infty$. $\mathbb{E} \left[\int_0^{t_0} \|\tilde{F}_t^{n,n} - F_t^n\|^2 dt \right]$ is the training loss (3.17) at level n .

Proof. We use Fubini's theorem and triangle inequality to derive

$$(3.30) \quad \int_0^{t_0} \mathbb{E}[\|\tilde{F}_t^{n,m} - F_t^m\|^2] dt \leq 3 \int_0^{t_0} \mathbb{E}[\|\tilde{F}_t^{n,m} - \tilde{F}_t^{n,n}\|^2] \\ + \mathbb{E}[\|\tilde{F}_t^{n,n} - F_t^n\|^2] + \mathbb{E}[\|F_t^n - F_t^m\|^2] dt.$$

First, we observe for the third term goes to zero uniformly in $m \geq n$ as $n \rightarrow \infty$ since F_t^n is assumed to converge and, in particular, is a Cauchy sequence, in the Bochner space $L^2(\Omega, \mathcal{F}, \mathbb{P}; L^2([0, t_0]; H))$. Then

$$(3.31) \quad \int_0^{t_0} \mathbb{E}[\|\tilde{F}_t^{n,m} - \tilde{F}_t^{n,n}\|^2] dt \leq (L_{t_0}^n)^2 \int_0^{t_0} \mathbb{E}[\|X_{T-t}^m - X_{T-t}^n\|^2] dt \\ \leq (L_{t_0}^n)^2 \int_0^{t_0} 2 a_{T-t}^{-2} \mathbb{E}[\|X_0^m - X_0^n\|^2] + 2(1 - a_{T-t}^{-2}) \text{tr}(Q_m - Q_n) dt \\ \leq 2 t_0 (L_{t_0}^n)^2 \left(\mathbb{E}[\|X_0^m - X_0^n\|^2] + \sum_{k=n+1}^m \lambda_k \right),$$

where the first inequality is by the Lipschitz continuity of \tilde{f}^n , and the second inequality is from (3.8). By assumption, $\mathbb{E}[\|X_0\|^2] < \infty$. Together with the fact that $L_{t_0}^n$ is bounded uniformly in n and Q is a trace class operator, this implies that the term goes to zero uniformly in $m \geq n$ as $n \rightarrow \infty$. \blacksquare

The convergence of $f^n(t, X_t^n)$ in $L^2(\Omega, \mathcal{F}, \mathbb{P}; L^2([0, t_0]; H))$ as assumed in the previous theorem is weaker than convergence $L^2(\Omega, \mathcal{F}, \mathbb{P}; \mathcal{C}([0, t_0]; H))$. Such uniform convergence of $f^n(t, X_t^n)$ is a reasonable assumption as is discussed in [43].

4. Multilevel Learning Approaches. Our discretization of the infinite-dimensional SBDM differs from most commonly used diffusion models in two aspects: First, we use a neural operator architecture to learn the score operator s_θ , for instance, FNO [38]; Second, we change the latent distribution \mathbb{P}_Z as well as the noise η in the loss function to a Gaussian noise with trace class covariance operator Q . Both of these choices are discussed in the next sections.

4.1. FNO parameterization of the score function. We use the Fourier neural operator (FNO) architecture [38] to render the score network, s_θ , resolution invariant. In the spirit of [35], we want to learn the score operator as a map between function spaces. However, since our viewpoint is finite-dimensional in training (we circumvent the definition of the infinite-dimensional score), we formulate this section in finite dimensions.

The input to our score operator $s_\theta^{\text{FNO}} : [0, T] \times \mathbb{R}^{n,n} \rightarrow \mathbb{R}^{n,n}$ are an image and time. To this end, we concatenate the image x with the time component and obtain $\tilde{x}_t = (x, t) \in \mathbb{R}^{2,n,n}$. The first channel is the image of size $n \times n$, and the second is a constant image whose value equals t . The score network is defined by the composition

$$s_\theta^{\text{FNO}}(\tilde{x}_t) = A \circ \mathcal{L}_L \circ \dots \circ \mathcal{L}_1 \circ R(\tilde{x}_t).$$

The lifting mapping, R , is parameterized by the neural network with $R(\tilde{x}_t)$ and increases the channel size, i.e., it is a map from $\mathbb{R}^{2,n,n} \rightarrow \mathbb{R}^{ch,n,n}$. Similarly, A reduces the feature map

to one channel. The layers \mathcal{L} are what make the FNO architecture resolution invariant. For simplicity, we define the operator for $\text{ch} = 1$ and refer to the original work for the full case. For any $\ell = 1, \dots, L$, these are given by

$$\mathcal{L}_\ell(v) = \sigma(W_\ell v + b_\ell + \mathcal{K}(f_{\theta_\ell})v).$$

Here, $\mathcal{K}(f_\theta)$ a convolution operator defined by the periodic function f_θ . Assuming periodic boundary conditions on the images, we can compute this efficiently in Fourier space

$$\mathcal{K}(f_\theta)v = \text{FFT}^{-1}(P_\theta \odot \text{FFT}(v)),$$

where \odot is the Hadamard product and the equality holds if P_θ are the eigenvalues of $\mathcal{K}(f_\theta)$, which can be computed via FFT. As suggested in [38], we directly parameterize the non-zero entries P_θ associated with low frequencies and impose conjugate symmetry to ensure that the linear operator is real-valued. We denote the non-zero Fourier modes by $k = (k_1, k_2)$ with $k_1 > k_{\max}$ or $k_2 > k_{\max}$. As shown in [35, Theorem 5], FNOs can approximate any continuous operator between Sobolev spaces to arbitrary accuracy when k_{\max} is sufficiently large.

4.2. Prior distributions. We outline the four prior distributions used in our experiments.

Firstly, the standard Gaussian distribution is what we consider as a benchmark in order to investigate the role of trace-class operators in multilevel training.

Secondly, we obtain the negative inverse Laplacian $-\Delta^{-1}$ as a covariance kernel by using the standard five-point stencil. Assuming periodic boundary conditions on the images, as explained in the previous section, we can compute the eigenvalues of the Laplacian, denoted by $\lambda(-\Delta)$, with FFT and efficiently invert it in Fourier space by

$$(4.1) \quad A_{\text{Lap}}(x) = \text{FFT}^{-1}((\lambda(-\Delta))^{-1/2} \odot \text{FFT}(x)),$$

to sample efficiently from $\mathcal{N}(0, -\Delta^{-1})$, by first sampling $x \sim \mathcal{N}(0, I)$ and computing. The distribution can be multiplied by a scalar γ . We discuss its selection in [subsection 5.1](#).

Thirdly, the FNO prior is implemented by a randomly initialized spectral convolution layer, and it is applied to a standard Gaussian. The main idea is to transfer images to the frequency domain and to apply a "low-pass" filter to these. First, we choose a maximum number of modes, apply the Fourier transform to our input image x , cut off (or set them to 0) all the modes of higher order, and perform a spectral convolution like in [38]. Experimentally, we randomly initialize φ and impose the conjugate symmetry, although it could also be learned. More concisely, we can sum it up via

$$A_{\text{FNO}}(x) = \text{FFT}^{-1}(\varphi \odot \text{FFT}(x)).$$

Finally, we propose a new prior that combines the FNO prior and Laplacian prior and reads $A_{\text{comb}} = A_{\text{FNO}} + \gamma A_{\text{Lap}}$. Here, the hyperparameter γ controls the influence of each of those priors. This yields a linear map. Therefore, applying A_{comb} to a standard Gaussian yields a Gaussian. Furthermore, the influence of the inverse Laplacian takes care that we indeed obtain a non-degenerate covariance. The main idea is to combine a "low-pass" filter and a trace class operator to satisfy both the theoretical requirement and the empirical performance, so a combined prior is not restricted to A_{comb} we propose.

Prior	Standard, Laplacian, FNO, Combined (scale $\gamma = \{1, 5, \mathbf{10}, 15\}$)	
Network	U-Net	FNO
Configuration	Channel = $\{32, \mathbf{64}\}$, Residual block count = $\{2, \mathbf{4}\}$	cutoff $k_{\max} = \{8, 12, 14, 15\}$, Layer 1 width = $\{\mathbf{64}, 128\}$, Layer 2 width = $\{64, \mathbf{128}\}$
Batch size	$\{128, \mathbf{256}, 512\}$	
Learning rate	$\{1e-3, \mathbf{1e-4}\}$	

Table 1: Hyperparameter space used in our grid search. The best hyperparameter values are marked in bold. The best k_{\max} values differ with the choice of priors, and is discussed in [subsection 5.1](#).

5. Experiments. We test our infinite-dimensional diffusion models for image generation using the MNIST and Fashion-MNIST [66] datasets. The python code is available at <https://github.com/PaulLyonel/multilevelDiff.git>. We show the benefits of multilevel learning with neural operator architectures and trace class covariance operators.

5.1. MNIST experiment. We interpolate the MNIST data to size 56×56 and split it into a training set of 50000 images and a validation set of 10000. Our models are trained on images of resolution 28×28 , obtained by average pooling, and validated on higher resolutions.

We employ a grid search method for hyperparameter tuning to optimize the performance of our model. The set of hyperparameters is listed in [Table 1](#). These are chosen based on prior knowledge and tests, as well as some common setups of U-Net in [28] and [30]. We choose the mode cutoff level $k_{\max} < \frac{n}{2} + 1$, where $n \times n$ is the size of the image. We conduct a separate training process for each candidate hyperparameter combination for 500 epochs with the Adam optimizer. Within each epoch, it iterates over the training dataset of resolution 28×28 and computes the loss. During the evaluation, we select the best hyperparameters for the eight model combinations (two network options and four priors); see Prior and Network row in [Table 1](#). We first pick the three best models in each of the eight model combinations with the lowest average Riesz MMD values of 56×56 resolution over the last 250 epochs. This indicates the ability to generalize to higher resolutions. The Riesz MMD [54] is particularly interesting because it is a two-sample test [60] also known as the energy distance, as it has metric properties and is particularly well suited for image generation [27]. From the subset of the three best-performing models, the final model is determined using visual perception of numeric recognizability as a criterion, mainly at higher resolution 56×56 .

Thus we obtain the best combination for each combination of networks and prior distributions. In [Table 2](#), we report the MMD values achieved by the generated images from the best setup for each combination of networks and prior distributions. Note that the MMD values are not always a perfect measure of the quality of the generated images.

As shown in [Figure 1](#), the FNO models trained on low-resolution images are superior at generating high-resolution images compared to the U-Net models. For the FNO architecture, one can also see some advantages of the FNO and combined prior. The standard Gaussian or Laplacian prior induce mode collapse in high resolution. This can be seen from the dominance of numbers 1 and 9 in standard Gaussian and the dominance of numbers 3 and 4

Prior	Standard Gaussian		Laplacian		FNO		Combined	
Network	U-Net	FNO	U-Net	FNO	U-Net	FNO	U-Net	FNO
MMD 28	0.0160	0.0124	0.0951	0.0402	0.0107	0.0079	0.0113	0.0101
MMD 56	2.5290	1.3295	2.4996	0.1987	2.1161	1.3931	2.1911	0.2136

Table 2: Comparison of the MMD values achieved by different priors and networks, in both resolutions 28 and 56, using 10000 test samples from the MNIST dataset.

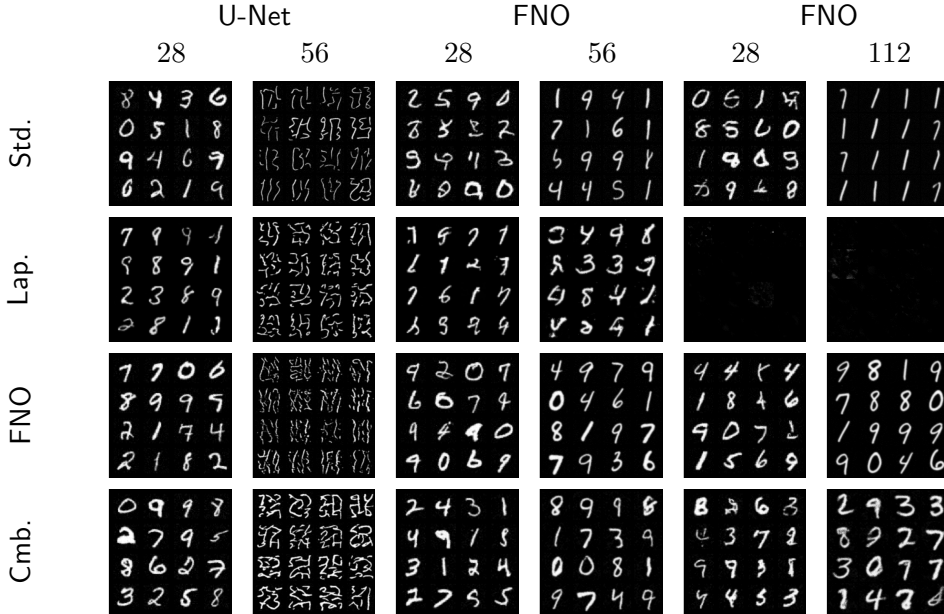


Figure 1: Comparison of U-Net and FNO architectures' generated image quality on resolutions 28 and 56. The last two columns show the generalizability of FNO architecture to resolution 112, when trained in resolution 28 solely and evaluated at resolution 112. The U-Net images at resolution 56 do not resemble any digits. Among the FNO images, the performance of standard Normal and Laplacian prior degrade significantly compared to resolution 56, while FNO and combined prior persist sensible and diverse images even at resolution 112.

in Laplacian of Figure 1(b). Furthermore, the Laplacian prior exhibits an unstable training process, contributing to the near-black images generated. The prior FNO performs better with a low mode cutoff level $k_{\max} = 8$. While the other nondegenerate priors perform better with $k_{\max} = 12$. The scaling factor γ in the trace class operator, as defined in subsection 4.2, plays an important role in model performance. One possible reason is that the choice of the scaling factor influences the extent of the smoothing applied to the image functions. In terms of the computation time, with combined prior, $k_{\max} = 12$, and the best configuration outlined in Table 1, U-Net architecture uses 9M parameters with 196 seconds per epoch, FNO

architecture uses 8M parameters with 60 seconds per epoch.

We investigate the ability of the FNO network trained on resolution 28×28 to generate realistic images of resolution 112×112 ; see [Figure 1](#). The mode collapse is aggravated in the standard Gaussian prior. The Laplacian prior generates a nearly black image, showing the challenge of multilevel training. However, FNO and the combined prior on resolution 112 preserve a good generating quality. The slight degradation in the image quality of the combined prior can potentially be improved with carefully chosen configurations on the scaling factor or alternative trace class priors. However, the images generated from the combined prior seem better at capturing different styles, such as boldness and slantedness.

5.2. Fashion-MNIST. We select hyperparameters and generate Fashion-MNIST images by following the same procedure as for the MNIST dataset. Again, all models are trained on resolution 28×28 and evaluated at higher resolution.

The results in [Figure 2](#) align with the previous experiment: the FNO architecture works better at generating high-resolution images and has the diversity to generate more than seven fashion categories. The FNO architecture with combined prior shows the capability of capturing more details and styles of the different classes in generated images. With a focus on resolution 56×56 images, the combined prior can generate images from all ten classes of fashion items. The FNO prior leads to a slight mode collapse on sandals. Standard Gaussian and Laplacian have one or two items in the generated images that are hard to recognize. The Laplacian prior is not stable during training in that the image quality does not maintain or improve along the training epochs. The Vendi diversity score [\[14\]](#) in [Figure 2](#) supports the advantage of the combined prior in capturing the different styles in generated classes. Since the combined prior has the highest diversity score in resolutions 28 and 56. Note that the diversity scores for the U-Net architecture at resolution 56 are not meaningful since the generated images do not resemble examples from the Fashion-MNIST dataset.

6. Discussion and Future Work. We analyze infinite-dimensional score-based generative models (SBDMs) for image generation and develop multilevel algorithms. Our theory underscores the importance of changing the latent distribution in existing SBDMs to trace class Gaussians. With this choice, we show the well-posedness of the resulting forward and reverse processes. We show that the discretizations of both processes converge to their continuous counterparts. We also present an explicit error estimate on the Wasserstein paths, which bounds the distance to the data distribution. In our numerical experiments, we compare different covariance operators and network architectures using the MNIST and Fashion-MNIST. While our work and related papers [\[34, 39, 43, 13\]](#) are important first steps towards well-posed infinite-dimensional SBDMs, more work is needed to achieve state-of-the-art results.

As our experiments and similar results in [\[13\]](#) suggest, investigating more advanced neural operator architectures can be a future research direction. In our work, the FNO model is better at generating smoother images. The low-frequency representation implied by the FNO does not necessarily need to be true for image distribution, since it cannot perfectly capture sharp edges in images. As possible alternatives, one may consider Wavelet neural operators [\[20\]](#), the U-Net neural operators [\[45\]](#), or modifying the U-Net architecture to enable multilevel training such as done in [\[65\]](#) to leverage the strong inductive bias of U-Nets. Furthermore, [\[22\]](#) argues that CNNs imply at least continuity of infinite-dimensional images, which also opens

	Std.	Lap.	FNO	Cmb.	
M.	1.27	1.30	1.49	1.27	28
D.	5.74	4.37	5.92	5.62	

	Std.	Lap.	FNO	Cmb.	
M.	2.08	7.49	2.80	7.02	56
D.	26.62	441.2	24.62	4.44	

(a) U-Net architecture

	Std.	Lap.	FNO	Cmb.	
M.	1.3 ± 0.01	1.9 ± 0.1	1.2 ± 0.1	1.3 ± 0.04	28
D.	6.0 ± 0.09	4.4 ± 0.3	8.7 ± 1.6	6.5 ± 0.13	

	Std.	Lap.	FNO	Cmb.	
M.	2.6 ± 0.09	2.7 ± 0.2	2.5 ± 0.1	2.3 ± 0.1	56
D.	6.0 ± 0.19	4.9 ± 0.2	5.9 ± 0.1	6.0 ± 0.1	

(b) FNO architecture

Figure 2: Comparison of the network architectures and the priors on resolution 28 and 56. In the tables, “M.” denotes the MMD values (lower is better) and “D.” denotes the Vendi diversity scores (higher is better) of their corresponding generated images. The diversity scores of resolution 56 under U-Net architecture are not meaningful since the generated images are not sensible. We further test the FNO architecture in 5 training runs with different random seed. The results are presented in the form of mean \pm standard error.

the possibility of more specialized theoretical analysis. We also note that there is a myriad of other trace class operators that may be more suitable for the SBDM problem. A possible reason for the unstable training behavior of Laplacian prior could be the noise schedule. The current noise schedule is more suitable for standard Gaussian, FNO, and the combined prior.

Our experiments suggest that an FNO architecture trained on a low resolution can yield a good warm start for higher resolutions. An open question in the training arises from the behavior of stochastic approximation methods, such as Adam, in the infinite-dimensional setting. Compared to the numerical optimization techniques in multilevel approaches for other variational problems (see, e.g., [42] for applications in image registration), those methods are not descent methods. Hence, depending on the learning rate, even a perfect initialization from coarse mesh training may not lead to convergence to a global minimum at the fine level.

7. Acknowledgements. PH thanks Chin-Wei Huang, Rafael Orozco, Jakiw Pidstrigach, and Shifan Zhao, and NY thanks Tomoyuki Ichiba and Nils Detering for helpful discussions.

REFERENCES

- [1] G. S. Alberti, M. Santacesaria, and S. Sciotto. Continuous generative neural networks. *arXiv 2205.14627*, 2023.
- [2] B. D. Anderson. Reverse-time diffusion equation models. *Stochastic Processes and their Applications*, 12(3):313–326, 1982.
- [3] L. Baldassari, A. Siahkoochi, J. Garnier, K. Solna, and M. V. de Hoop. Conditional score-based diffusion models for bayesian inference in infinite dimensions, 2023.
- [4] G. Batzolis, J. Stanczuk, C.-B. Schönlieb, and C. Etmann. Non-uniform diffusion models. *arXiv:2207.09786*, 2022.
- [5] S. Bond-Taylor and C. G. Willcocks. Inf-diff: Infinite resolution diffusion with subsampled mollified states. *CoRR*, 2023.
- [6] R. Carmona. *Lectures on BSDEs, stochastic control, and stochastic differential games with financial applications*. SIAM, 2016.
- [7] T. F. Chan, J. Shen, and L. Vese. Variational PDE models in image processing. *Notices AMS*, 50(1):14–26, 2003.
- [8] R. T. Chen, Y. Rubanova, J. Bettencourt, and D. K. Duvenaud. Neural ordinary differential equations. *Advances in neural information processing systems*, 31, 2018.
- [9] G. Da Prato and J. Zabczyk. *Stochastic Equations in Infinite Dimensions*. Cambridge University Press, 2014.
- [10] E. Dupont, Y. W. Teh, and A. Doucet. Generative models as distributions of functions. *arXiv:2102.04776*, 2021.
- [11] W. E. A Proposal on Machine Learning via Dynamical Systems. *Communications in Mathematics and Statistics*, 2017.
- [12] E. Emmrich. *Gewöhnliche und Operator-Differentialgleichungen*. Vieweg Teubner Verlag, 2004.
- [13] G. Franzese, S. Rossi, D. Rossi, M. Heinonen, M. Filippone, and P. Michiardi. Continuous-time functional diffusion processes. *arXiv:2303.00800*, 2023.
- [14] D. Friedman and A. B. Dieng. The vendi score: A diversity evaluation metric for machine learning. *arXiv preprint arXiv:2210.02410*, 2022.
- [15] H. Föllmer and A. Wakolbinger. Time reversal of infinite-dimensional diffusions. *Stochastic Processes and their Applications*, 22(1):59–77, 1986.
- [16] J.-F. L. Gall. *Brownian Motion, Martingales, and Stochastic Calculus*. Springer Publishing Company, Incorporated, 2018.
- [17] L. Gawarecki and V. Mandrekar. *Stochastic Differential Equations in Infinite Dimensions*. Probability and Its Applications. Springer, Berlin, Heidelberg, 2010.
- [18] L. Gawarecki and V. Mandrekar. *Stochastic differential equations in infinite dimensions: with applications to stochastic partial differential equations*. Springer Science & Business Media, 2010.
- [19] T. H. Gronwall. Note on the derivatives with respect to a parameter of the solutions of a system of differential equations. *Annals of Mathematics*, 20(4):292–296, 1919.
- [20] G. Gupta, X. Xiao, and P. Bogdan. Multiwavelet-based operator learning for differential equations. In A. Beygelzimer, Y. Dauphin, P. Liang, and J. W. Vaughan, editors, *Advances in Neural Information Processing Systems*, 2021.
- [21] E. Haber and L. Ruthotto. Stable architectures for deep neural networks. *Inverse Problems*, 34(1):014004, 2017. Supported by NSF DMS 1522599.
- [22] A. Habring and M. Holler. A note on the regularity of images generated by convolutional neural networks. *SIAM Journal on Mathematics of Data Science*, 5(3):670–692, 2023.
- [23] P. Hagemann, J. Hertrich, and G. Steidl. Stochastic normalizing flows for inverse problems: A Markov chain viewpoint. *SIAM Journal on Uncertainty Quantification*, 10:1162–1190, 2022.
- [24] P. Hagemann, J. Hertrich, and G. Steidl. *Generalized normalizing flows via Markov chains*. Elements in Non-local Data Interactions: Foundations and Applications. Cambridge University Press, 2023.
- [25] M. Hairer. An introduction to stochastic PDEs. *arXiv*, 2009.
- [26] U. G. Haussmann and E. Pardoux. Time reversal of diffusions. *The Annals of Probability*, pages 1188–1205, 1986.
- [27] J. Hertrich, C. Wald, F. Altekrieger, and P. Hagemann. Generative sliced mmd flows with riesz kernels.

- arXiv:2305.11463*, 2023.
- [28] J. Ho, A. Jain, and P. Abbeel. Denoising diffusion probabilistic models. In H. Larochelle, M. Ranzato, R. Hadsell, M. Balcan, and H. Lin, editors, *Advances in Neural Information Processing Systems*, volume 33, pages 6840–6851. Curran Associates, Inc., 2020.
- [29] E. Hoogeboom, J. Heek, and T. Salimans. simple diffusion: End-to-end diffusion for high resolution images. *arXiv:2301.11093*, 2023.
- [30] C.-W. Huang, J. H. Lim, and A. C. Courville. A variational perspective on diffusion-based generative models and score matching. In M. Ranzato, A. Beygelzimer, Y. Dauphin, P. Liang, and J. W. Vaughan, editors, *Advances in Neural Information Processing Systems*, volume 34, pages 22863–22876. Curran Associates, Inc., 2021.
- [31] A. Hyvärinen. Estimation of non-normalized statistical models by score matching. *Journal of Machine Learning Research*, 6(24):695–709, 2005.
- [32] T. Ichiba and T. Yang. Relative arbitrage opportunities in n investors and mean-field regimes. *arXiv:2006.15158*, 2020.
- [33] T. Karras, T. Aila, S. Laine, and J. Lehtinen. Progressive growing of GANs for improved quality, stability, and variation. In *International Conference on Learning Representations*, 2018.
- [34] G. Kerrigan, J. Ley, and P. Smyth. Diffusion generative models in infinite dimensions. *arXiv:2212.00886*, 2022.
- [35] N. Kovachki, S. Lanthaler, and S. Mishra. On universal approximation and error bounds for Fourier neural operators. *The Journal of Machine Learning Research*, 22(1):13237–13312, 2021.
- [36] V. Kulikov, S. Yadin, M. Kleiner, and T. Michaeli. Sinddm: A single image denoising diffusion model. *arXiv:2211.16582*, 2022.
- [37] S. Lee, H. Chung, J. Kim, and J. C. Ye. Progressive deblurring of diffusion models for coarse-to-fine image synthesis. *arXiv:2207.11192*, 2022.
- [38] Z. Li, N. Kovachki, K. Azizzadenesheli, B. Liu, K. Bhattacharya, A. Stuart, and A. Anandkumar. Fourier neural operator for parametric partial differential equations, 2020.
- [39] J. H. Lim, N. B. Kovachki, R. Baptista, C. Beckham, K. Azizzadenesheli, J. Kossaifi, V. Voleti, J. Song, K. Kreis, J. Kautz, C. Pal, A. Vahdat, and A. Anandkumar. Score-based diffusion models in function space. *arXiv:2302.07400*, 2023.
- [40] W. Liu and M. Röckner. *Stochastic Partial Differential Equations: an Introduction*. Springer, 2015.
- [41] A. Millet, D. Nualart, and M. Sanz. Time reversal for infinite-dimensional diffusions. *Probability theory and related fields*, 82(3):315–347, 1989.
- [42] J. Modersitzki. *FAIR: flexible algorithms for image registration*, volume 6 of *Society for Industrial and Applied Mathematics (SIAM), Philadelphia, PA*. Society for Industrial and Applied Mathematics (SIAM), Philadelphia, PA, 2009.
- [43] J. Pidstrigach, Y. Marzouk, S. Reich, and S. Wang. Infinite-dimensional diffusion models for function spaces. *arXiv:2302.10130*, 2023.
- [44] M. A. Rahman, M. A. Florez, A. Anandkumar, Z. E. Ross, and K. Azizzadenesheli. Generative adversarial neural operators. *Transactions on Machine Learning Research*, 2022.
- [45] M. A. Rahman, Z. E. Ross, and K. Azizzadenesheli. U-NO: U-shaped neural operators, 2022.
- [46] S. Rissanen, M. Heinonen, and A. Solin. Generative modelling with inverse heat dissipation. *arXiv:2206.13397*, 2022.
- [47] M. Röckner, B. Schmuland, and X. Zhang. Yamada-watanabe theorem for stochastic evolution equations in infinite dimensions. *Condensed Matter Physics*, 11, 2008.
- [48] R. Rombach, A. Blattmann, D. Lorenz, P. Esser, and B. Ommer. High-resolution image synthesis with latent diffusion models. In *Proceedings of the IEEE Conference on Computer Vision and Pattern Recognition (CVPR)*, 2022.
- [49] F. Russo and P. Vallois. *Stochastic Calculus via Regularizations*. Bocconi & Springer Series. Springer Cham, 2022.
- [50] L. Ruthotto and E. Haber. Deep neural networks motivated by partial differential equations. *Journal of Mathematical Imaging and Vision*, 62:352–364, 2020.
- [51] M. Scheutzow. Stochastic partial differential equations, 2019. <https://page.math.tu-berlin.de/~scheutzow/SPDEmain.pdf>.
- [52] M. Scheutzow. Stochastic processes iii/wahrscheinlichkeitstheorie iv, 2019. <https://page.math.tu-berlin>.

de/~scheutzow/WT4main.pdf.

- [53] R. L. Schilling and L. Partzsch. *Brownian motion: an introduction to stochastic processes*. Walter de Gruyter GmbH & Co KG, 2014.
- [54] D. Sejdinovic, B. Sriperumbudur, A. Gretton, and K. Fukumizu. Equivalence of distance-based and RKHS-based statistics in hypothesis testing. *The Annals of Statistics*, 41(5):2263 – 2291, 2013.
- [55] J. Sohl-Dickstein, E. Weiss, N. Maheswaranathan, and S. Ganguli. Deep unsupervised learning using nonequilibrium thermodynamics. In F. Bach and D. Blei, editors, *Proceedings of the 32nd International Conference on Machine Learning*, volume 37 of *Proceedings of Machine Learning Research*, pages 2256–2265, Lille, France, 07–09 Jul 2015. PMLR.
- [56] Y. Song, C. Durkan, I. Murray, and S. Ermon. Maximum likelihood training of score-based diffusion models. In A. Beygelzimer, Y. Dauphin, P. Liang, and J. W. Vaughan, editors, *Advances in Neural Information Processing Systems*, 2021.
- [57] Y. Song and S. Ermon. Generative modeling by estimating gradients of the data distribution. In H. Wallach, H. Larochelle, A. Beygelzimer, F. d’Alché Buc, E. Fox, and R. Garnett, editors, *Advances in Neural Information Processing Systems*, volume 32. Curran Associates, Inc., 2019.
- [58] Y. Song, J. Sohl-Dickstein, D. P. Kingma, A. Kumar, S. Ermon, and B. Poole. Score-based generative modeling through stochastic differential equations. *arXiv*, 2020.
- [59] A. M. Stuart. Inverse problems: A Bayesian perspective. *Acta Numerica*, 19:451–559, May 2010.
- [60] G. J. Székely and M. L. Rizzo. Energy statistics: A class of statistics based on distances. *Journal of Statistical Planning and Inference*, 143(8):1249–1272, 2013.
- [61] R. Vershynin. *High-dimensional Probability: An Introduction with Applications in Data Science*, volume 47. Cambridge University Press, 2018.
- [62] C. Villani et al. *Optimal transport: old and new*, volume 338. Springer, 2009.
- [63] P. Vincent. A connection between score matching and denoising autoencoders. *Neural Comput.*, 23(7):1661–1674, jul 2011.
- [64] V. Voleti, C. Pal, and A. Oberman. Score-based denoising diffusion with non-isotropic gaussian noise models. *arXiv:2210.12254*, 2022.
- [65] C. Williams, F. Falck, G. Deligiannidis, C. Holmes, A. Doucet, and S. Syed. A unified framework for u-net design and analysis. *arXiv 2305.19638*, 2023.
- [66] H. Xiao, K. Rasul, and R. Vollgraf. Fashion-mnist: a novel image dataset for benchmarking machine learning algorithms. 2017.

Appendix A. Hilbert Space Valued Wiener Processes. This section is based on [9, 25, 51, 40]. Let H be a separable Hilbert space and $\mathcal{B}(H)$ its Borel σ -algebra. By $L(H)$ we denote the space of bounded linear operators and by $K(H)$ the subspace of compact operators mapping from H to H . Further, let H^* be the dual space of bounded linear functionals from H to \mathbb{R} . By Riesz’ representation theorem, there exists an isomorphism between H^* and H , more precisely every linear bounded functional corresponds to an element $v \in H$ by $\ell_v(u) = \langle u, v \rangle$ for all $u \in H$. Let $(e_k)_{k \in \mathbb{N}}$ be an orthonormal basis of H . A self-adjoint, positive semidefinite operator $Q \in L(H)$ which satisfies

$$\text{tr}(Q) := \sum_{k=1}^{\infty} \langle Qe_k, e_k \rangle < \infty$$

is called *trace class* (operator) with trace $\text{tr}(Q)$. The definition is independent of the chosen basis. Trace class operators are in particular compact operators and Hilbert-Schmidt operators. Recall that for two separable Hilbert spaces H_1 and H_2 , a linear bounded operator $T : H_1 \rightarrow H_2$ is called a *Hilbert-Schmidt operator* if

$$\|T\|_{L_2(H_1, H_2)} := \left(\sum_{k=1}^{\infty} \langle \|Te_k\|_{H_2}^2 \rangle \right)^{\frac{1}{2}} < \infty,$$

for an orthonormal basis $(e_k)_{k \in \mathbb{N}}$ of H_1 . The space $L_2(H_1, H_2)$ of all such operators with the above norm is again a Hilbert space.

Let $(\Omega, \mathcal{F}, \mathbb{P})$ be a probability space where Ω is a nonempty set and \mathcal{F} is a σ -algebra of subsets of Ω . For a Banach space E , we denote by $L^2(\Omega, \mathcal{F}, \mathbb{P}; E)$, the Bochner space of measurable functions $f : \Omega \rightarrow E$ with norm

$$\|f\|_{L^2(\Omega, \mathcal{F}, \mathbb{P}; E)} := \left(\int_{\Omega} \|f\|_E^2 d\mathbb{P} \right)^{\frac{1}{2}} < \infty.$$

Often, we consider the case $E = \mathcal{C}([0, T], H)$, which we always equip with the uniform norm.

A measure μ on $(H, \mathcal{B}(H))$ is called *Gaussian* if $\ell_{\#}\mu := \mu \circ \ell^{-1}$ is a Gaussian measure on \mathbb{R} for all $\ell \in H^*$. An H -valued *random variable* $X : \Omega \rightarrow H$ is called *Gaussian* if $\mu = X_{\#}\mathbb{P}$ is a Gaussian measure on H . By the following theorem [51, Theorem 3.12], there is a one-to-one correspondence between Gaussian measures and pairs (m, Q) , where $m \in H$ and $Q \in K(H)$ is trace class.

Theorem A.1. *A measure μ on $(H, \mathcal{B}(H))$ is Gaussian if and only if there exists some $m \in H$ and some trace class operator $Q \in K(H)$ such that*

$$(A.1) \quad \hat{\mu}(u) := \int_H e^{i\langle u, v \rangle} d\mu(v) = e^{i\langle m, u \rangle - \frac{1}{2}\langle Qu, u \rangle}, \quad u \in H.$$

Then $m \in H$ is called the *mean* of μ and $Q \in K(H)$ *covariance (operator) of μ* and we write $\mathcal{N}(m, Q)$ instead of μ and $X \sim \mathcal{N}(m, Q)$ for the corresponding random variable. The Gaussian measure determines m and Q uniquely, and conversely, for each (m, Q) , $m \in H$, $Q \in K(H)$ trace class, there exists a Gaussian measure which fulfills (A.1). Furthermore, the following relations hold true for all $v, \tilde{v} \in H$:

- i) $\int_H \langle u, v \rangle d\mu(u) = \langle m, v \rangle$,
- ii) $\int_H (\langle u, v \rangle - \langle m, v \rangle) (\langle u, \tilde{v} \rangle - \langle m, \tilde{v} \rangle) d\mu(u) = \langle Q\tilde{v}, v \rangle$,
- iii) $\int_H \|u - m\|^2 d\mu(u) = \text{tr}(Q)$,
and similarly for the corresponding random variable
- iv) $\mathbb{E}(\langle X, v \rangle) = \langle m, v \rangle$,
- v) $\text{Cov}(\langle X, v \rangle, \langle X, \tilde{v} \rangle) = \langle Q\tilde{v}, v \rangle$,
- vi) $\mathbb{E}(\|X - m\|^2) = \text{tr}(Q)$.

Now let $(e_k)_{k \in \mathbb{N}}$ be an orthonormal basis of eigenvectors of a trace class operator $Q \in K(H)$ with eigenvalues $\lambda_1 \geq \lambda_2 \geq \dots \geq 0$. Then $X \sim \mathcal{N}(m, Q)$ if and only if

$$(A.2) \quad X = m + \sum_{k \in \mathbb{N}_Q} \sqrt{\lambda_k} \beta_k e_k,$$

where β_k , $k \in \mathbb{N}_Q := \{j \in \mathbb{N} : \lambda_j > 0\}$, are independent $\mathcal{N}(0, 1)$ distributed random variables. The series converges in $L^2(\Omega, \mathcal{F}, \mathbb{P}; H)$ [51, Theorem 3.15].

For a trace class operator $Q \in K(H)$ and $T > 0$, a H -valued random process $W^Q = (W_t^Q)_{t \in [0, T]}$ is called a *Q-Wiener process* if $W_0^Q = 0$, W has continuous trajectories and independent increments, and fulfills for $t, s \in [0, T]$ the relation

$$W_t^Q - W_s^Q \sim \mathcal{N}(0, (t - s)Q) \quad \text{for all } 0 \leq s \leq t \leq T.$$

Let $(e_k)_{k \in \mathbb{N}}$ be an orthonormal basis of eigenfunctions of Q corresponding to eigenvalues $(\lambda_k)_{k \in \mathbb{N}}$. By [51, Theorem 3.17] an H -valued random process W^Q on $(\Omega, \mathcal{F}, \mathbb{P})$ is a Q -Wiener process if and only if there exist mutually independent standard Wiener processes $(\beta_k)_{k \in \mathbb{N}}$ on $(\Omega, \mathcal{F}, \mathbb{P})$ such that

$$(A.3) \quad W_t^Q = \sum_{k \in \mathbb{N}} \sqrt{\lambda_k} \beta_k(t) e_k,$$

where the series on the right-hand side, the so-called *Karhunen–Loève decomposition* of W^Q , is convergent in $L^2(\Omega, \mathcal{F}, \mathbb{P}; \mathcal{C}([0, T], H))$.

For fixed $T > 0$, a *filtration* $\mathbb{F} = (\mathcal{F}_t)_{t \in [0, T]}$ on $(\Omega, \mathcal{F}, \mathbb{P})$ is called *complete* if \mathcal{F}_0 contains all $A \subset \Omega$ such that $A \subset B$ for some $B \in \mathcal{F}$ such with $\mathbb{P}(B) = 0$. The *completion* of a filtration \mathbb{F} is the smallest complete filtration containing \mathbb{F} . The filtration is called *right-continuous* if $\mathcal{F}_t = \bigcap_{s > t} \mathcal{F}_s$ for all $t \in [0, T]$ and a complete and right-continuous filtration is called *normal*. A Q -Wiener process W^Q is a Q -Wiener process with respect to \mathbb{F} , if W^Q is \mathbb{F} adapted and $W_t^Q - W_s^Q$ is independent of \mathcal{F}_s for all $0 \leq s \leq t \leq T$. Every Q -Wiener process is such a process with respect to some normal filtration; e.g., the completion of the filtration generated by W^Q . Note that this filtration is always right-continuous due to the continuity of sample paths of W^Q .

Stochastic integrals with respect to W^Q can be introduced in a very similar way to the classical finite-dimensional case. First, one defines integrals for elementary functions with values in the space of Hilbert-Schmidt operators $L_2(H_Q, K)$, where $H_Q := Q^{\frac{1}{2}}H$ denotes the Cameron-Martin space of Q and K is some separable Hilbert space. Then one extends the stochastic integral via the Itô isometry [17, Eq. (2.19)]

$$\mathbb{E} \left[\left\| \int_0^t \phi(s) dW_s^Q \right\|_K^2 \right] = \mathbb{E} \left[\int_0^t \|\phi(s)\|_{L_2(Q^{\frac{1}{2}}H, K)}^2 ds \right],$$

to adapted $L_2(H_Q, K)$ -valued processes ϕ for which the right-hand side is finite. With this isometry at hand, the integral is finally defined for the larger class of adapted $L_2(H_Q, K)$ -valued processes with almost surely square integrable Hilbert-Schmidt norm. For more details, we refer to [9, 17, 40].

Appendix B. Complete Proofs. This supplementary provides the proof of [Theorem 3.1](#) and more detailed proofs of [Theorem 3.4](#) and [Theorem 3.6](#).

B.1. Proof of [Theorem 3.1](#).

Proof. 1. First, we show the existence and uniqueness of a strong solution of [\(3.2\)](#). We verify that the assumptions of [17, Thm. 3.3] are satisfied. We start by noting that the measurability assumptions of the theorem are trivially satisfied in our setting since our drift and diffusion coefficients f and g are deterministic, i.e., they do not depend on the probability space $(\Omega, \mathcal{F}, \mathbb{P})$, and continuous on $[0, T] \times H$ and $[0, T]$, respectively. Furthermore, we have the linear growth bound

$$\|f(t, x)\| + \|g(t)\|_{L_2(H_Q, H)} \leq \left(\frac{1}{2} \|\alpha\|_{\mathcal{C}([0, T], \mathbb{R})} + \sqrt{\|\alpha\|_{\mathcal{C}([0, T], \mathbb{R})} \operatorname{tr}(Q)} \right) (1 + \|x\|)$$

and the Lipschitz condition

$$\|f(t, x_1) - f(t, x_2)\| \leq \frac{1}{2} \|\alpha\|_{\mathcal{C}([0, T], \mathbb{R})} \|x_1 - x_2\|.$$

Thus, we can apply [17, Thm. 3.3] and conclude that (3.2) has a unique strong solution $(X_t)_{t \in [0, T]}$ which satisfies $\mathbb{E} \left[\sup_{t \in [0, T]} \|X_t\|^2 \right] < \infty$ if $\mathbb{E} [\|X_0\|^2] < \infty$.

2. Next, we prove that $(X_t)_{t \in [0, T]}$ is given by (3.3). For $k \in \mathbb{N}$, we define

$$F^k: [0, T] \times H \rightarrow \mathbb{R}, \quad F^k(t, x) := a_t \langle x, e_k \rangle.$$

Clearly, F^k is continuous with Fréchet partial derivatives $F_x^k(t, x) = a_t e_k$, $F_{xx}^k(t, x) = 0$, and $F_t^k(t, x) = \frac{1}{2} \alpha_t a_t \langle x, e_k \rangle$ that are continuous and bounded on bounded subsets of $[0, T] \times H$. Let $(X_t)_{t \in [0, T]}$ be the unique strong solution of (3.2). We obtain by Itô's formula [17, Thm. 2.9] \mathbb{P} -almost surely for all $t \in [0, T]$ that

(B.1)

$$F^k(t, X_t) = F^k(0, X_0) + \int_0^t \langle F_x^k(s, X_s), \sqrt{\alpha_s} dW_s^Q \rangle + \int_0^t \left(F_t^k(s, X_s) + \langle F_x^k(s, X_s), -\frac{1}{2} \alpha_s X_s \rangle + \frac{1}{2} \text{tr}(F_{xx}^k(s, X_s) \sqrt{\alpha_s} Q) \right) ds$$

(B.2)

$$(B.3) \quad = \langle X_0, e_k \rangle + \int_0^t \langle a_s e_k, \sqrt{\alpha_s} dW_s^Q \rangle,$$

with

$$(B.4) \quad \begin{aligned} \int_0^t \langle a_s e_k, \sqrt{\alpha_s} dW_s^Q \rangle &:= \int_0^t a_s \sqrt{\alpha_s} \langle e_k, \cdot \rangle dW_s^Q \\ &= \sum_{k'=1}^{\infty} \int_0^t a_s \sqrt{\alpha_s} \langle e_k, e_{k'} \rangle d\langle W_s^Q, e_{k'} \rangle \\ &= \sqrt{\lambda_k} \int_0^t a_s \sqrt{\alpha_s} d\beta_k(s), \end{aligned}$$

where the first equality is the definition of the left-hand side and the second equality follows from [17, Lem. 2.8]. On the other hand, by [17, Ex. 2.9], we have \mathbb{P} -almost surely

$$\left\langle \int_0^t a_s \sqrt{\alpha_s} dW_s^Q, e_k \right\rangle = \sqrt{\lambda_k} \int_0^t a_s \sqrt{\alpha_s} d\beta_k(s), \quad t \in [0, T].$$

Overall, we obtain \mathbb{P} -almost surely for all $k \in \mathbb{N}$ that

$$\langle X_t, e_k \rangle = a_t^{-1} \left(\langle X_0, e_k \rangle + \left\langle \int_0^t a_s \sqrt{\alpha_s} dW_s^Q, e_k \right\rangle \right),$$

which proves (3.3).

3. Finally, we consider B_t in (3.4). By [17, Lem. 2.8], we immediately obtain

$$B_t = \sum_{k \in \mathbb{N}} \sqrt{\lambda_k} \left(\int_0^t a_s \sqrt{\alpha_s} d\beta_k(s) \right) e_k$$

in $L^2(\Omega, \mathcal{F}, \mathbb{P}; H)$ for all $t \in [0, T]$. By construction of the stochastic integral, the difference

$$\delta B_t^K := B_t - \sum_{k=1}^K \sqrt{\lambda_k} \left(\int_0^t a_s \sqrt{\alpha_s} d\beta_k(s) \right) e_k \in L^2(\Omega, \mathcal{F}, \mathbb{P}; H)$$

is an H -valued square-integrable martingale for all $K \in \mathbb{N}$ and thus, by Doob's maximal inequality [17, Thm. 2.2],

$$\mathbb{E} \left[\sup_{t \in [0, T]} \|\delta B_t^K\|^2 \right] \leq 4 \mathbb{E} \left[\|\delta B_T^K\|^2 \right] \rightarrow 0 \text{ as } K \rightarrow \infty,$$

which proves the second part of (3.4). For $k \in \mathbb{N}$, we set

$$b_k(t) := \int_0^t a_s \sqrt{\alpha_s} d\beta_k(s), \quad t \in [0, T].$$

In the finite-dimensional setting it is well-known that the stochastic integral of a deterministic function with respect to a Brownian motion is a centered Gaussian, see e.g. [16, p. 108]. In particular $b_k(t)$ is a centered Gaussian for all $k \in \mathbb{N}$ and all $t \in [0, T]$. By the Itô isometry, we obtain

$$(B.5) \quad \text{Var} [b_k(t)] = \mathbb{E} \left[\left(\int_0^t a_s \sqrt{\alpha_s} d\beta_k(s) \right)^2 \right] = \int_0^t a_s^2 \alpha_s ds = a_t^2 - 1.$$

For $t > 0$, we have $(a_t^2 - 1)^{-1/2} b_k(t) \sim \mathcal{N}(0, 1)$ for all $k \in \mathbb{N}$ and by (3.4) it holds

$$(B.6) \quad B_t = \sum_{k \in \mathbb{N}} \sqrt{\lambda_k (a_t^2 - 1)} (a_t^2 - 1)^{-1/2} b_k(t) e_k$$

in $L^2(\Omega, \mathcal{F}, \mathbb{P}; H)$. By [51, Thm. 3.15], we obtain that B_t is a centered $(a_t^2 - 1)Q$ -Gaussian, since $((a_t^2 - 1)^{-1/2} b_k(t))_{k \in \mathbb{N}}$ are mutually independent. \blacksquare

B.2. Proof of Theorem 3.4.

Proof. 1. First, we show that p_t^n has the form (3.13) which then implies that f^n in (3.14) is well-defined with the desired properties. By Theorem 3.1, we know that B_t^n in (3.7) is a centered Gaussian in H_n with covariance $(a_t^2 - 1)Q_n$ and thus \hat{B}_t^n is a centered Gaussian in \mathbb{R}^n with covariance $(a_t^2 - 1)\text{diag}(\lambda_1, \dots, \lambda_n)$. In particular, for all $t \in (0, T]$,

$$\hat{b}_t^n(z) := \frac{(\lambda_1 \dots \lambda_n)^{-1/2}}{(2\pi(a_t^2 - 1))^{n/2}} b_t^n(z)$$

is the Lebesgue density of \hat{B}_t^n , cf. e.g. [16, Thm 1.3]. By (3.7), we have

$$\hat{X}_t^n = a_t^{-1} (\hat{X}_0^n + \hat{B}_t^n), \quad t \in [0, T].$$

Since X_0^n and B_t^n are independent, \hat{X}_0^n and \hat{B}_t^n are also independent and thus their sum $\hat{X}_0^n + \hat{B}_t^n$ has density $p_0^n * \hat{b}_t^n$ for all $t \in (0, T]$. By scaling we see that \hat{X}_t^n has the density

$$p_t^n(z) := \frac{a_t^n (\lambda_1 \dots \lambda_n)^{-1/2}}{(2\pi(a_t^2 - 1))^{n/2}} (p_0^n * b_t^n)(a_t z).$$

For $t \in (0, T]$, we observe that b_t^n is twice continuously differentiable and it holds

$$\partial_k b_t^n(z) = -(a_t^2 - 1)^{-1} (\lambda_k)^{-1} z_k b_t^n(z), \quad k = 1, \dots, n,$$

and

$$\partial_\ell (\partial_k b_t^n)(z) = \begin{cases} (a_t^2 - 1)^{-2} (\lambda_\ell)^{-1} (\lambda_k)^{-1} z_\ell z_k b_t^n(z), & \ell \neq k \\ (a_t^2 - 1)^{-2} (\lambda_k)^{-2} z_k^2 b_t^n(z) - (a_t^2 - 1)^{-1} (\lambda_k)^{-1} b_t^n(z), & \ell = k. \end{cases}$$

Clearly, we have $\partial_k b_t^n \in L^1(\mathbb{R}^n)$ and $\partial_\ell \partial_k b_t^n \in L^1(\mathbb{R}^n)$ and therefore $\partial_k (p_0^n * b_t^n) = p_0^n * (\partial_k b_t^n)$ and $\partial_\ell \partial_k (p_0^n * b_t^n) = p_0^n * (\partial_\ell \partial_k b_t^n)$. In particular, p_t^n is twice continuously differentiable with

$$\partial_k p_t^n(z) = -\frac{a_t^{n+1} (\lambda_k)^{-1} (\lambda_1 \dots \lambda_n)^{-1/2}}{(a_t^2 - 1) (2\pi(a_t^2 - 1))^{n/2}} (p_0^n * (z_k b_t^n))(a_t z), \quad k = 1, \dots, n,$$

and

$$\partial_\ell \partial_k p_t^n(z) = -\frac{a_t^{n+2} (\lambda_1 \dots \lambda_n)^{-1/2}}{(2\pi(a_t^2 - 1))^{n/2}} (p_0^n * \partial_\ell \partial_k b_t^n)(a_t z), \quad \ell, k \in \{1, \dots, n\}.$$

As it is convolution of a probability density function and a strictly positive function, we have $(p_0^n * b_t^n)(z) > 0$ and thus also $p_t^n(z) > 0$ for all $z \in \mathbb{R}^n$. The chain rule yields

$$\nabla \log p_t^n(z) = \frac{\nabla p_t^n(z)}{p_t^n(z)} = -\frac{a_t}{(a_t^2 - 1)} \left(\frac{(\lambda_k)^{-1} (p_0^n * \cdot_k b_t^n)(a_t z)}{(p_0^n * b_t^n)(a_t z)} \right)_{k=1}^n,$$

which is (3.11), and

$$\nabla^2 \log p_t^n(z) = \frac{\nabla^2 p_t^n(z)}{p_t^n(z)} - \frac{\nabla p_t^n(z) \nabla p_t^n(z)^\top}{p_t^n(z)^2}.$$

Since all terms are continuous in $z \in \mathbb{R}^n$ and $t \in (0, T]$, we conclude that $\nabla^2 \log p_t^n$ is bounded on $[\delta, T] \times \{z \in \mathbb{R}^n \mid \|z\| \leq N\}$ for all $\delta > 0$ and $N \in \mathbb{N}$. Thus, the function f^n as in (3.13) is well-defined and Lipschitz continuous in the second variable uniformly on $[0, T - \delta] \times \{x \in H_n \mid \|x\| \leq N\}$.

2. Next, we transfer (3.5) to an SDE on \mathbb{R}^n to obtain a reverse equation. Let $\beta_k(t)$, $k \in \mathbb{N}$

be as in (A.3). Then the process $\beta_t^n := (\beta_k(t))_{k=1}^n$ is an n -dimensional Brownian motion and $(\hat{X}_t^n)_{t \in [0, T]}$ is the unique strong solution of

$$d\hat{X}_t^n = -\frac{1}{2}\alpha_t \hat{X}_t^n dt + \sqrt{\alpha_t} \text{diag}(\sqrt{\lambda_1}, \dots, \sqrt{\lambda_n}) d\beta_t^n$$

with initial value \hat{X}_0^n . We can verify that for all $\delta > 0$ and all bounded open sets $U \subset \mathbb{R}^n$

$$(B.7) \quad \int_{\delta}^T \int_U |p_t^n(z)|^2 + \alpha_t \lambda_k |\partial_k p_t^n(z)|^2 dz dt < \infty, \quad k = 1, \dots, n.$$

By [26, Thm 2.1] we conclude that the time reversal $(\hat{X}_{T-t}^n)_{t \in [0, T]}$ is a solution of the martingale problem, cf. [52, Section 3.3], associated to the reverse SDE

$$(B.8) \quad d\hat{Y}_t^n = \left(\frac{1}{2}\alpha_{T-t} \hat{Y}_t^n + \alpha_{T-t} \text{diag}(\lambda_1, \dots, \lambda_k) \nabla \log p_{T-t}^n(\hat{Y}_t^n) \right) dt + \sqrt{\alpha_{T-t}} \text{diag}(\sqrt{\lambda_1}, \dots, \sqrt{\lambda_n}) d\hat{\beta}_t^n$$

with initial condition $\hat{Y}_0^n \sim \mathbb{P}_{\hat{X}_T^n}$. Let \mathbb{F} be the completion of the natural filtration of $(X_{T-t}^n)_{t \in [0, T]}$. It is well-known that solutions of martingale problems correspond to weak solutions of the associated SDE. In particular, by [52, Thm 3.15], there is a weak solution $((\hat{\Omega}, \hat{\mathcal{F}}, \hat{\mathbb{F}}, \hat{\mathbb{P}}), (\hat{Y}_t^n)_{t \in [0, T]}, \hat{\beta}^n)$ of (B.8) such that $(\hat{\Omega}, \hat{\mathcal{F}}, \hat{\mathbb{F}}, \hat{\mathbb{P}})$ is an extension of $(\Omega, \mathcal{F}, \mathbb{F}, \mathbb{P})$ and $(\hat{Y}_t^n)_{t \in [0, T]}$ is the canonical extension of $(\hat{X}_{T-t}^n)_{t \in [0, T]}$ to $(\hat{\Omega}, \hat{\mathcal{F}}, \hat{\mathbb{F}}, \hat{\mathbb{P}})$, cf. [52, Def. 3.13]. Thus, $(\hat{Y}_t^n)_{t \in [0, T]}$ is equal to $(\hat{X}_{T-t}^n)_{t \in [0, T]}$ in distribution. Since $\hat{\beta}^n$ is an n -dimensional Brownian motion, we have $\hat{\beta}_t^n = (\hat{\beta}_k^n(t))_{k=1}^n$ for some mutually independent standard Brownian motions $(\hat{\beta}_k^n(t))_{k=1}^n$. Therefore, the process

$$\hat{W}_t^{Q_n} := \sum_{k=1}^n \sqrt{\lambda_k} \hat{\beta}_k^n(t) e_k$$

is a Q_n -Wiener process on $(\hat{\Omega}, \hat{\mathcal{F}}, \hat{\mathbb{F}}, \hat{\mathbb{P}})$. We set $Y_t^n := \iota_n^{-1}(\hat{Y}_t^n)$. Clearly, $(Y_t^n)_{t \in [0, T]}$ and $(X_{T-t}^n)_{t \in [0, T]}$ are equal in distribution. Since $((\hat{\Omega}, \hat{\mathcal{F}}, \hat{\mathbb{F}}, \hat{\mathbb{P}}), (\hat{Y}_t^n)_{t \in [0, T]}, \hat{\beta}^n)$ is a weak solution of (B.8), the process $(Y_t^n)_{t \in [0, T]}$ has continuous sample-paths and is adapted to $\hat{\mathbb{F}}$. Further,

since Y_t^n fulfills (3.1) for the setting (B.8), we have $\hat{\mathbb{P}}$ -almost surely for all $t \in [0, T]$ that (B.9)

$$\begin{aligned}
Y_t^n &= \sum_{k=1}^n \left((\hat{Y}_0^n)_k + \int_0^t \frac{1}{2} \alpha_{T-s} (\hat{Y}_s^n)_k + \alpha_{T-s} \lambda_k \partial_k \log p_{T-s}^n (\hat{Y}_s^n) ds \right. \\
&\quad \left. + \int_0^t \sqrt{\alpha_{T-s}} \sqrt{\lambda_k} d\hat{\beta}_k^n(s) \right) e_k \\
&= \iota_n^{-1} (\hat{Y}_0^n) + \int_0^t \frac{1}{2} \alpha_{T-s} \iota_n^{-1} (\hat{Y}_s^n) + \alpha_{T-s} Q_n \left(\sum_{k=1}^n \partial_k \log p_{T-s}^n (\iota_n (\iota_n^{-1} (\hat{Y}_s^n))) e_k \right) ds \\
&\quad + \int_0^t \sqrt{\alpha_{T-s}} d\hat{W}_s^{Q_n} \\
&= Y_0^n + \int_0^t \frac{1}{2} \alpha_{T-s} Y_s^n + \underbrace{\alpha_{T-s} Q_n (\iota_n^{-1} \circ \nabla \log p_{T-t}^n \circ \iota_n) (Y_s^n)}_{=f^n(s, Y_s^n)} ds + \int_0^t \sqrt{\alpha_{T-s}} d\hat{W}_s^{Q_n},
\end{aligned}$$

and thus $((\hat{\Omega}, \hat{\mathcal{F}}, \hat{\mathbb{F}}, \hat{\mathbb{P}}), (Y_t^n)_{t \in [0, T]}, \hat{W}^{Q_n})$ is a weak solution of (3.14) with $Y_0^n \sim \mathbb{P}_{X_T^n}$. Starting with a weak solution $((\hat{\Omega}, \hat{\mathcal{F}}, \hat{\mathbb{F}}, \hat{\mathbb{P}}), (Y_t^n)_{t \in [0, T]}, \hat{W}^{Q_n})$ of (3.14), we can analogously show that $((\hat{\Omega}, \hat{\mathcal{F}}, \hat{\mathbb{F}}, \hat{\mathbb{P}}), (\hat{Y}_t^n)_{t \in [0, T]}, \hat{\beta}^n)$ with $\hat{Y}_t^n := \iota_n(Y_t^n)$ and $\hat{\beta}_t^n := ((\sqrt{\lambda_k})^{-1} \langle \hat{W}_t^{Q_n}, e_k \rangle)_{k=1}^n$ yields a weak solution of (B.8). Thus, showing uniqueness in law of (B.8) is sufficient to prove uniqueness in law of (3.14). Because the drift and diffusion coefficients of (B.8) are Lipschitz continuous in the second variable on sets of the form $[0, T - \delta] \times \{z \in \mathbb{R}^n \mid \|z\| \leq N\}$, we know by [49, Lem. 12.4] and [49, Definition 12.1] that pathwise uniqueness holds on $[0, T - \delta]$, i.e., any two weak solutions on $[0, T - \delta]$ that are defined on the same filtered probability space with the same Brownian motion are indistinguishable. A limiting argument $\delta \rightarrow 0$ yields pathwise uniqueness on $[0, T]$. It is a classical result by Yamada and Watanabe [49, Prop. 13.1] that pathwise uniqueness implies uniqueness in law.

Finally, we note that by Theorem 3.1 the forward process satisfies $\mathbb{E}[\sup_{t \in [0, T]} \|X_t^n\|^2] < \infty$. As we have proven that any weak solution $((\hat{\Omega}, \hat{\mathcal{F}}, \hat{\mathbb{F}}, \hat{\mathbb{P}}), (Y_t^n)_{t \in [0, T]}, \hat{W}^{Q_n})$ of (3.14) is equal to $(X_{T-t}^n)_{t \in [0, T]}$ in distribution, this immediately implies $\mathbb{E}[\sup_{t \in [0, T]} \|Y_t^n\|^2] < \infty$. ■

B.3. Proof of Theorem 3.6. We will need the fact that the Wasserstein-2 distance metrizes weak convergence in those spaces [62, Thm 6.9]. More precisely, we have for a sequence $(\mu_n)_n$ that $W_2(\mu_n, \mu) \rightarrow 0$ as $n \rightarrow \infty$ if and only if $\int_K \varphi d\mu_n \rightarrow \int_K \varphi d\mu$ for all $\varphi \in C_b(K)$ and $\int_K d(x_0, x)^2 d\mu_n \rightarrow \int_X d(x_0, x)^2 d\mu$ for any $x_0 \in K$ as $n \rightarrow \infty$.

To prepare Theorem 3.6, we need the following lemma.

Lemma B.1 (Gronwall's inequality [12, 19]). *Let $h \in L^\infty([0, t_0])$ for some $t_0 > 0$. Assume that there exist $a \geq 0$ and $b > 0$ such that $h(t) \leq a + b \int_0^t h(s) ds$ for all $t \in [0, t_0]$. Then it holds*

$$h(t) \leq a e^{bt}, \quad t \in [0, t_0].$$

Now we can prove the theorem.

Proof. 1. First, we observe that since by assumption \tilde{f}^n is continuous $[0, t_0] \times H$ and Lipschitz continuous in the second variable, we can apply [18, Thm 3.3] to conclude that for

any initial condition and Q_n -Wiener process independent of the initial condition the SDE (3.16) has a unique strong solution on $[0, t_0]$. Note that the existence of a unique strong solution implies that solutions are unique in law [47, Remark 1.10]. In particular, the measure $\mathbb{P}_{(\tilde{Y}_t^n)_{t_0}}$ is well-defined. We use $\mathbb{P}_{(\check{Y}_t^n)_{t_0}}$ to denote the path measure induced by (3.16), but with initial distribution $\mathbb{P}_{X_T^n}$. Then we obtain by the triangle inequality

$$\begin{aligned} W_2(\mathbb{P}_{(X_{T-t}^n)_{t_0}}, \mathbb{P}_{(\tilde{Y}_t^n)_{t_0}}) &\leq W_2(\mathbb{P}_{(X_{T-t}^n)_{t_0}}, \mathbb{P}_{(Y_t^n)_{t_0}}) + W_2(\mathbb{P}_{(Y_t^n)_{t_0}}, \mathbb{P}_{(\check{Y}_t^n)_{t_0}}) \\ &\quad + W_2(\mathbb{P}_{(\check{Y}_t^n)_{t_0}}, \mathbb{P}_{(\tilde{Y}_t^n)_{t_0}}), \\ W_2^2(\mathbb{P}_{(X_{T-t}^n)_{t_0}}, \mathbb{P}_{(\tilde{Y}_t^n)_{t_0}}) &\leq 4W_2^2(\mathbb{P}_{(X_{T-t}^n)_{t_0}}, \mathbb{P}_{(Y_t^n)_{t_0}}) \\ &\quad + 2W_2^2(\mathbb{P}_{(Y_t^n)_{t_0}}, \mathbb{P}_{(\check{Y}_t^n)_{t_0}}) + 4W_2^2(\mathbb{P}_{(\check{Y}_t^n)_{t_0}}, \mathbb{P}_{(\tilde{Y}_t^n)_{t_0}}). \end{aligned}$$

By [Theorem 3.4](#), the first term is zero.

2. Next, we bound the third term. Let \check{Y}_0^n and \tilde{Y}_0^n be any realizations of $\mathbb{P}_{X_T^n}$ and $\mathcal{N}(0, Q_n)$, respectively, that are defined on the same probability space. For some driving Q_n -Wiener process independent of \check{Y}_0^n and \tilde{Y}_0^n and defined on the same probability space (or possibly an extension of it), let $(\check{Y}_t^n)_{t \in [0, t_0]}$ and $(\tilde{Y}_t^n)_{t \in [0, t_0]}$ be the unique strong solutions of (3.16) started from \check{Y}_0^n and \tilde{Y}_0^n , respectively. By (3.1) and using Jensen's inequality, we obtain for $s \in [0, t_0]$,

$$\begin{aligned} \|\check{Y}_s^n - \tilde{Y}_s^n\|^2 &\leq 3 \left(\|\check{Y}_0^n - \tilde{Y}_0^n\|^2 + \left\| \int_0^s \frac{1}{2} \alpha_{T-r} (\check{Y}_r^n - \tilde{Y}_r^n) dr \right\|^2 \right. \\ &\quad \left. + \left\| \int_0^s \tilde{f}^n(r, \check{Y}_r^n) - \tilde{f}^n(r, \tilde{Y}_r^n) dr \right\|^2 \right) \\ &\leq 3 \left(\|\check{Y}_0^n - \tilde{Y}_0^n\|^2 + s \int_0^s \left\| \frac{1}{2} \alpha_{T-r} (\check{Y}_r^n - \tilde{Y}_r^n) \right\|^2 dr \right. \\ &\quad \left. + s \int_0^s \|\tilde{f}^n(r, \check{Y}_r^n) - \tilde{f}^n(r, \tilde{Y}_r^n)\|^2 dr \right) \\ &\leq 3 \|\check{Y}_0^n - \tilde{Y}_0^n\|^2 + 3t_0 \sup_{r \in [0, t_0]} \left(\frac{\alpha_{T-r}^2}{4} + (L_r^n)^2 \right) \int_0^s \|\check{Y}_r^n - \tilde{Y}_r^n\|^2 dr. \end{aligned}$$

Setting $h_1(t) := \mathbb{E}[\sup_{s \in [0, t]} \|\check{Y}_s^n - \tilde{Y}_s^n\|^2]$ for $t \in [0, t_0]$, we consequently obtain

$$\begin{aligned} h_1(t) &\leq 3\mathbb{E}[\|\check{Y}_0^n - \tilde{Y}_0^n\|^2] + 3t_0 \xi(t_0) \mathbb{E} \left[\sup_{s \in [0, t]} \int_0^s \|\check{Y}_r^n - \tilde{Y}_r^n\|^2 dr \right] \\ &\leq 3\mathbb{E}[\|\check{Y}_0^n - \tilde{Y}_0^n\|^2] + 3t_0 \xi(t_0) \mathbb{E} \left[\int_0^t \|\check{Y}_r^n - \tilde{Y}_r^n\|^2 dr \right] \\ &\leq 3\mathbb{E}[\|\check{Y}_0^n - \tilde{Y}_0^n\|^2] + 3t_0 \xi(t_0) \int_0^t h_1(r) dr, \end{aligned}$$

where we used Fubini's theorem for the last inequality. By [Theorem 3.1](#), the discretized forward process satisfies $\mathbb{E}[\sup_{t \in [T-t_0, T]} \|X_t^n\|^2] < \infty$ and in particular $\mathbb{E}[\|\check{Y}_0^n\|^2] = \mathbb{E}[\|X_T^n\|^2] < \infty$. By [Theorem A.1](#)(vi), we also have $\mathbb{E}[\|\tilde{Y}_0^n\|^2] = \text{tr}(Q_n) < \infty$. Together with [18, Thm 3.3],

we can argue that for every $t \in [0, t_0]$ it holds

$$h_1(t) = \mathbb{E} \left[\sup_{s \in [0, t]} \|\check{Y}_s^n - \tilde{Y}_s^n\|^2 \right] \leq 2 \mathbb{E} \left[\sup_{s \in [0, t_0]} \|\check{Y}_s^n\|^2 \right] + 2 \mathbb{E} \left[\sup_{s \in [0, t_0]} \|\tilde{Y}_s^n\|^2 \right] < \infty,$$

so that $h_1 \in L^\infty([0, t_0])$. Thus, we can apply Gronwall's lemma to h_1 and obtain for all $t \in [0, t_0]$ that

$$h_1(t) \leq 3 \mathbb{E} [\|\check{Y}_0^n - \tilde{Y}_0^n\|^2] e^{3\xi(t_0)t_0 t}.$$

In particular, the Wasserstein-2 distance can be estimated by

$$\begin{aligned} W_2^2(\mathbb{P}_{(\check{Y}_t^n)_{t_0}}, \mathbb{P}_{(\tilde{Y}_t^n)_{t_0}}) &\leq \mathbb{E} \left[\sup_{s \in [0, t_0]} \|\check{Y}_s^n - \tilde{Y}_s^n\|^2 \right] = h_1(t_0) \\ &\leq 3 e^{3\xi(t_0)t_0^2} \inf_{\substack{\check{Y}_0^n \sim \mathbb{P}_{X_T^n} \\ \tilde{Y}_0^n \sim \mathcal{N}(0, Q_n)}} \mathbb{E} [\|\check{Y}_0^n - \tilde{Y}_0^n\|^2] \\ &= 3 e^{3\xi(t_0)t_0^2} W_2^2(\mathbb{P}_{X_T^n}, \mathcal{N}(0, Q_n)), \end{aligned}$$

where we used that the previous estimates are valid for an arbitrary realization of \check{Y}_0^n and \tilde{Y}_0^n .
3. It remains to bound $W_2(\mathbb{P}_{(Y_t^n)_{t_0}}, \mathbb{P}_{(\check{Y}_t^n)_{t_0}})$. We pick a coupling for the probabilistic notion of the Wasserstein distance. By [Theorem 3.4](#), there exists a weak solution

$$((\hat{\Omega}, \hat{\mathcal{F}}, \hat{\mathbb{P}}, \hat{\mathbb{P}}), (Y_t^n)_{t \in [0, t_0]}, \hat{W}^{Q_n})$$

of the discretized reverse SDE [\(3.14\)](#) with initial condition $Y_0^n \sim \mathbb{P}_{X_T^n}$ such that $(\hat{\Omega}, \hat{\mathcal{F}}, \hat{\mathbb{P}}, \hat{\mathbb{P}})$ is an extension of $(\Omega, \mathcal{F}, \mathbb{P}, \mathbb{P})$ and $(Y_t^n)_{t \in [0, t_0]}$ is the canonical extension of $(X_{T-t}^n)_{t \in [0, t_0]}$ to this extended probability space. We define $(\check{Y}_t^n)_{t \in [0, t_0]}$ as the strong solution of the approximate reverse [\(3.16\)](#) with initial condition $\check{Y}_0^n = Y_0^n$ and the same driving noise \hat{W}^{Q_n} . As before, we can bound the difference as follows for $s \in [0, t_0]$:

$$\begin{aligned} \|Y_s^n - \check{Y}_s^n\|^2 &\leq \left\| Y_0^n - \check{Y}_0^n + \int_0^s \frac{1}{2} \alpha_{T-r} (Y_r^n - \check{Y}_r^n) dr + \int_0^s f^n(r, Y_r^n) - \tilde{f}^n(r, \check{Y}_r^n) dr \right\|^2 \\ &\leq 2t_0 \sup_{r \in [0, t_0]} \frac{\alpha_{T-r}^2}{4} \int_0^s \|Y_r^n - \check{Y}_r^n\|^2 dr + 2t_0 \int_0^s \|f^n(r, Y_r^n) - \tilde{f}^n(r, \check{Y}_r^n)\|^2 dr. \end{aligned}$$

For the second term we apply again the triangle inequality and obtain

$$\begin{aligned} &2t_0 \int_0^s \|f^n(r, Y_r^n) - \tilde{f}^n(r, \check{Y}_r^n)\|^2 dr \\ &\leq 4t_0 \int_0^s \|f^n(r, Y_r^n) - \tilde{f}^n(r, Y_r^n)\|^2 dr + 4t_0 \int_0^s \|\tilde{f}^n(r, Y_r^n) - \tilde{f}^n(r, \check{Y}_r^n)\|^2 dr \\ &\leq 4t_0 \int_0^s \|f^n(r, Y_r^n) - \tilde{f}^n(r, Y_r^n)\|^2 dr + 4t_0 \sup_{r \in [0, t_0]} (L_r^n)^2 \int_0^s \|Y_r^n - \check{Y}_r^n\|^2 dr. \end{aligned}$$

Since $(Y_t^n)_{t \in [0, t_0]}$ is an extension of $(X_{T-t}^n)_{t \in [0, t_0]}$, we obtain from assumption (3.17) that

$$\mathbb{E} \left[\sup_{t \in [0, s]} \int_0^s \|f^n(r, Y_r^n) - \tilde{f}^n(r, Y_r^n)\|^2 dr \right] \leq \mathbb{E} \left[\int_0^{t_0} \|f^n(r, Y_r^n) - \tilde{f}^n(r, Y_r^n)\|^2 dr \right] \leq \varepsilon.$$

We set $h_2(t) := \mathbb{E} [\sup_{s \in [0, t]} \|Y_s^n - \check{Y}_s^n\|^2]$ for $t \in [0, t_0]$ and get similarly as in the previous calculations

$$h_2(t) \leq 4t_0 \xi(t_0) \int_0^t h_2(s) ds + 4t_0 \varepsilon.$$

Since $(Y_t^n)_{t \in [0, t_0]}$ is equal to $(X_{T-t}^n)_{t \in [0, t_0]}$ in distribution and $\mathbb{E} [\sup_{t \in [0, T]} \|X_t^n\|^2] < \infty$ by [Theorem 3.1](#), we conclude

$$h_2(t) = \mathbb{E} \left[\sup_{s \in [0, t]} \|Y_s^n - \check{Y}_s^n\|^2 \right] \leq 2 \mathbb{E} \left[\sup_{s \in [0, t_0]} \|Y_s^n\|^2 \right] + 2 \mathbb{E} \left[\sup_{s \in [0, t_0]} \|\check{Y}_s^n\|^2 \right] < \infty, \quad t \in [0, t_0]$$

and thus $h_2 \in L^\infty([0, t_0])$. Now Gronwall's lemma applied to h_2 yields

$$W_2^2(\mathbb{P}_{(Y_t^n)_{t_0}}, \mathbb{P}_{(\check{Y}_t^n)_{t_0}}) \leq h_2(t_0) \leq 4t_0 \varepsilon e^{4\xi(t_0)t_0^2}.$$

In summary, we obtain

$$W_2^2(\mathbb{P}_{(X_{T-t}^n)_{t_0}}, \mathbb{P}_{(\tilde{Y}_t^n)_{t_0}}) \leq 12 \left(t_0 \varepsilon e^{4\xi(t_0)t_0^2} + e^{3\xi(t_0)t_0^2} W_2^2(\mathbb{P}_{X_T^n}, \mathcal{N}(0, Q_n)) \right). \quad \blacksquare$$

Appendix C. Hyperparameters.

C.1. MNIST. In [Table 2](#), we report the MMD values achieved by the generated images from the best setup for each combination of networks and prior distributions. The test set uses 10000 test samples in 28×28 and 56×56 resolutions. As explained in MNIST experiment setup, the MMD values are used as an initial screening, and the final setup for the eight models is determined by the image quality. The minimum MMD values can differ from the image quality we see in [Figure 1](#).

C.2. Fashion-MNIST. There are 10 classes in Fashion-MNIST images. Class 0-9 represents t-shirt, trousers, pullover, dress, coat, sandal, shirt, sneaker, bag, ankle boot, respectively.

We simplify the grid search of hyperparameters in Fashion-MNIST by utilizing the knowledge we get in MNIST's grid search. We emphasize on searching the scale γ and the mode cutoff k_{\max} , as can be seen in [Table 3](#). The best hyperparameters value is similar to what we select for MNIST experiment. Here, the mode cutoff is generally higher than MNIST. $k_{\max} = 15$ works the best for the combined prior, and $k_{\max} = 14$ works better for the rest. The scale factor $\gamma = 10$ in trace class operator remains to be the most suitable level, while $\gamma = 5$ and $\gamma = 12$ also behave roughly on par in terms of the image quality.

Category	Hyperparameters	
Prior	Standard, Laplacian, FNO, Combined (scale $\gamma = \{5, 10, 12, 15\}$)	
Network	U-Net	FNO
Configuration	Channel = {32, 64}, Residual block count={2, 4}	cutoff $k_{\max} = \{8, 12, 14, 15\}$, Layer 1 width = 64, Layer 2 width = 128
Batch size	256	
Learning rate	{1e-3, 1e-4}	

Table 3: Hyperparameter space used in grid search of Fashion-MNIST experiment.